

QUANTITATIVE STUDIES OF THE CALCAREOUS NANNOPLANKTON OF SARMATIAN DEPOSITS: CASE STUDIES IN THE SIENIAWA–RUDKA AREA (OUTER CARPATHIAN FOREDEEP, POLAND)

Dominika LELEK, Marta OSZCZYPKO-CLOWES & Nestor OSZCZYPKO

Institute of Geological Sciences, Jagiellonian University, Oleandry 2a, 30-063 Kraków, Poland; e-mails: dominika.lelek@uj.edu.pl; m.oszczypko-clowes@uj.edu.pl; nestor.oszczypko@uj.edu.pl

Lelek, D., Oszczypko-Clowes, M. & Oszczypko, N., 2016. Quantitative studies of the calcareous nannoplankton of Sarmatian deposits: case studies in the Sieniawa–Rudka area (Outer Carpathian Foredeep, Poland). *Annales Societatis Geologorum Poloniae*, 86: 29–57.

Abstract: The aim of this study was the qualitative and quantitative analysis of the calcareous nannofossil assemblages of the Machów Formation, belonging to the supra-evaporitic complex of the Polish Carpathian Foredeep Basin (PCFB). The work was concentrated in the eastern part of the PCFB, in the Sieniawa–Rudka area (Ryszkowa Wola Horst). Samples were collected from the Rudka-13 and Wylewa-1 boreholes. On the basis of calcareous nannoplankton, these deposits were assigned to the upper part of the NN6 Zone combined with the NN7 Zone, which corresponds to the Sarmatian *s.s.* of the Central Paratethys (upper Serravallian of the Mediterranean scale). Conclusive determination of the biozone NN7 was problematic, owing to the absence of the rare zonal marker species *Discoaster kugleri*. The typical association of the undivided NN6–NN7 Zone was of low species diversity and usually dominated by *Coccolithus pelagicus*, *Cyclicargolithus floridanus* and *Reticulofenestra pseudoumbilica* ($> 7 \mu\text{m}$). On the basis of the relative abundance of species, a significant amount of redeposition was deduced. The reworked nannofossils were mostly Eocene in age. The Oligocene, Early Miocene and Late Cretaceous species occurred much less frequently. The dominance of Eocene forms indicates the Carpathians as the main supply area. The Late Cretaceous taxa may have originated from the Senonian marly deposits of the Miechów Trough in the north. Statistical treatment of the quantitative data was performed using multivariate cluster analysis and Nonmetrical Multidimensional Scaling (nMDS). The composition of the calcareous nannofossil assemblages, together with the high percentage of allochthonous taxa, indicate a shallow, coastal environment with a high supply of nutrients.

Key words: Calcareous nannoplankton, biostratigraphy, palaeoenvironment, multivariate analysis, Sarmatian, Polish Carpathian Foredeep.

Manuscript received 9 October 2014, accepted 13 January 2016

INTRODUCTION

The late Badenian and Sarmatian succession in the NE part of the Polish Carpathian Foredeep Basin (PCFB), more than a kilometre thick, is predominantly composed of fine-grained, poorly consolidated, siliciclastic deposits, belonging to the Machów Formation. In the Central Paratethys, the late Badenian (early Serravallian) was the last period of fully marine conditions (Kováč *et al.*, 2007), during which a short-lived connection between the Central and Eastern Paratethys was re-established (Studencka and Jasionowski, 2011, and references therein). The late Badenian (Kosovian) transgression was related to the last, but very intense phase of the PCFB subsidence, which ended ca. 10.5 Ma (Oszczypko *et al.*, 2006). At the Badenian-Sarmatian boundary, the open ocean connections of the Central Paratethys were severely restricted, which caused a faunal re-orienta-

tion (Piller *et al.*, 2007). During the Sarmatian, the Central Paratethys become almost completely sealed off from the Mediterranean, but was well connected to the Eastern Paratethys (Rögl, 1998; Piller *et al.*, 2007; Studencka and Jasionowski, 2011). Towards the end of the Middle Miocene, the eastern Carpathian Foreland changed from the geo- and hydrodynamic regime of the Central Paratethys to that of the Eastern Paratethys (Piller *et al.*, 2007).

The objective of this research was the biostratigraphic and palaeoecological interpretation of the Machów Fm in the north-eastern part of the PCFB (Sieniawa–Rudka area, Ryszkowa Wola Horst), on the basis of calcareous nannofossil assemblages from the Wylewa-1 (W-1) and Rudka-13 (R-13) boreholes. Recently, the Machów Fm deposits in this area were intensively studied by Krzywiec *et al.* (2005) and

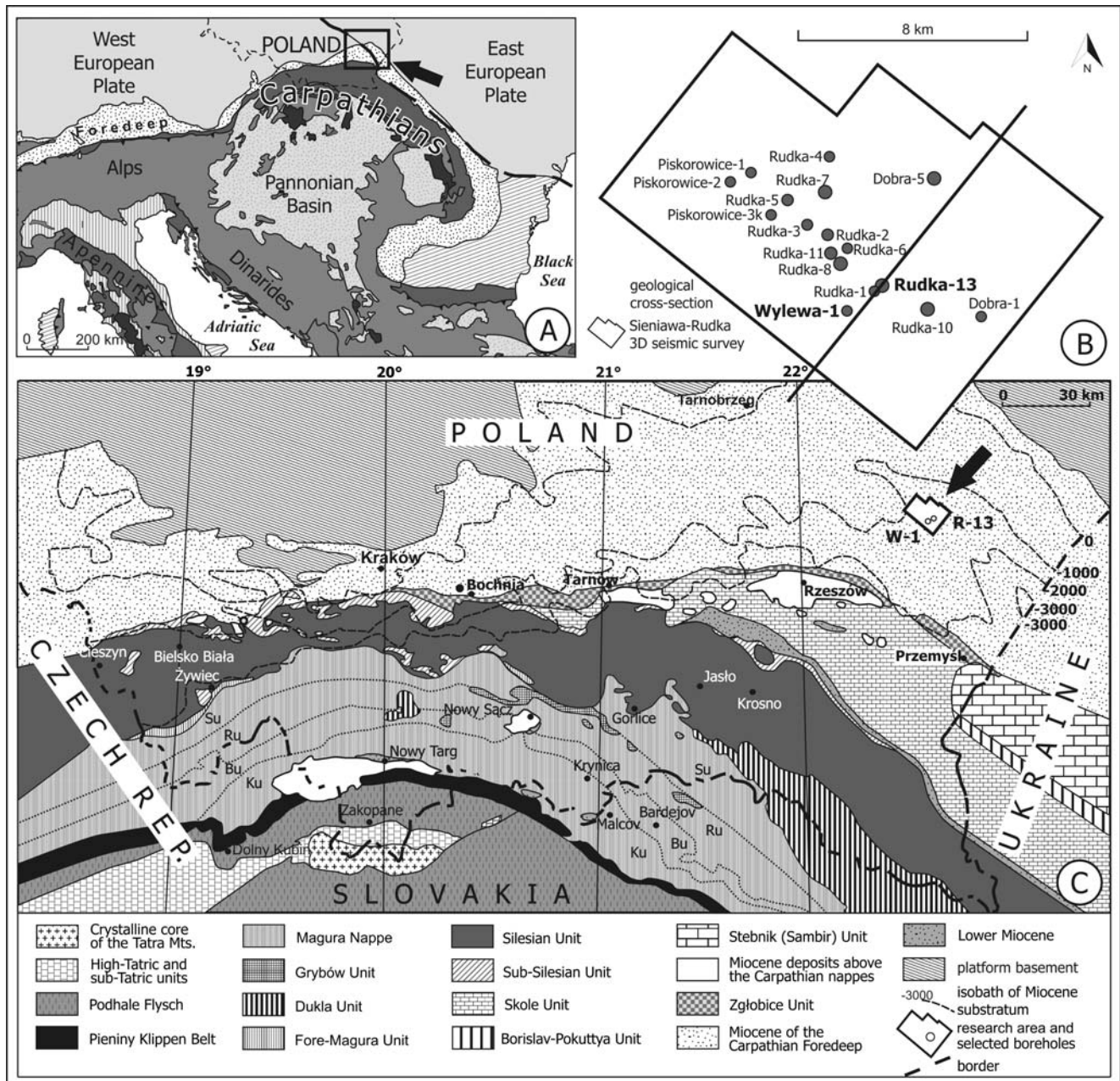


Fig. 1. Location maps. **A.** Position of the Polish Carpathian Foredeep in the Alpine-Carpathian system (after Oszczytko *et al.*, 2006, modified). **B.** Locality of wells on 3-D seismic image (investigated in this study bolded). **C.** Sketch-map of the Polish Carpathians and their foredeep (after Oszczytko 2006, modified). Abbreviations: Su – Siary, Ru – Rača, Bu – Bystrica, Ku – Krynica subunits of the Magura Nappe. Boreholes: P–3k (Piskorowice–3k), R–13 (Rudka–13). Main groups of tectonic units of the Outer Western Carpathians: Marginal Group (external): Borislav-Pokuttya, Stebnyk (Sambir) and Zgłobice Units; Middle Group (central): Grybów, Fore-Magura, Dukla, Silesian, Subsilesian and Skole units and Magura Group (internal).

Mastalerz *et al.* (2006). The primary aim of the present work was the estimation of quantitative relations between autochthonous and allochthonous assemblages of calcareous nannoplankton. The approximate percentage of the allochthonous group is an important component in the assessment of the intensity of erosion in the supply areas (i.e. the European Platform and the Carpathian orogen). These areas strongly differ in geological structure and in the ages of calcareous nannoplankton, with Mesozoic associations occurring on the platform and Palaeogene in the Flysch Carpathians.

GEOLOGICAL SETTING

The PCFB (Fig. 1), about 320 km long and up 100 km wide, is a part of the Alpine foreland basin system. It developed as a northern peripheral basin, related to the overthrusting Carpathian front (see Oszczytko, 1998, 1999; Oszczytko *et al.*, 2006). It is predominantly filled with marine clastic sediments of Miocene age, up to 3 km thick. The basement of the Carpathian Foredeep represents the epi-Variscan platform with its Mesozoic cover (Oszczytko, 2006). Ac-

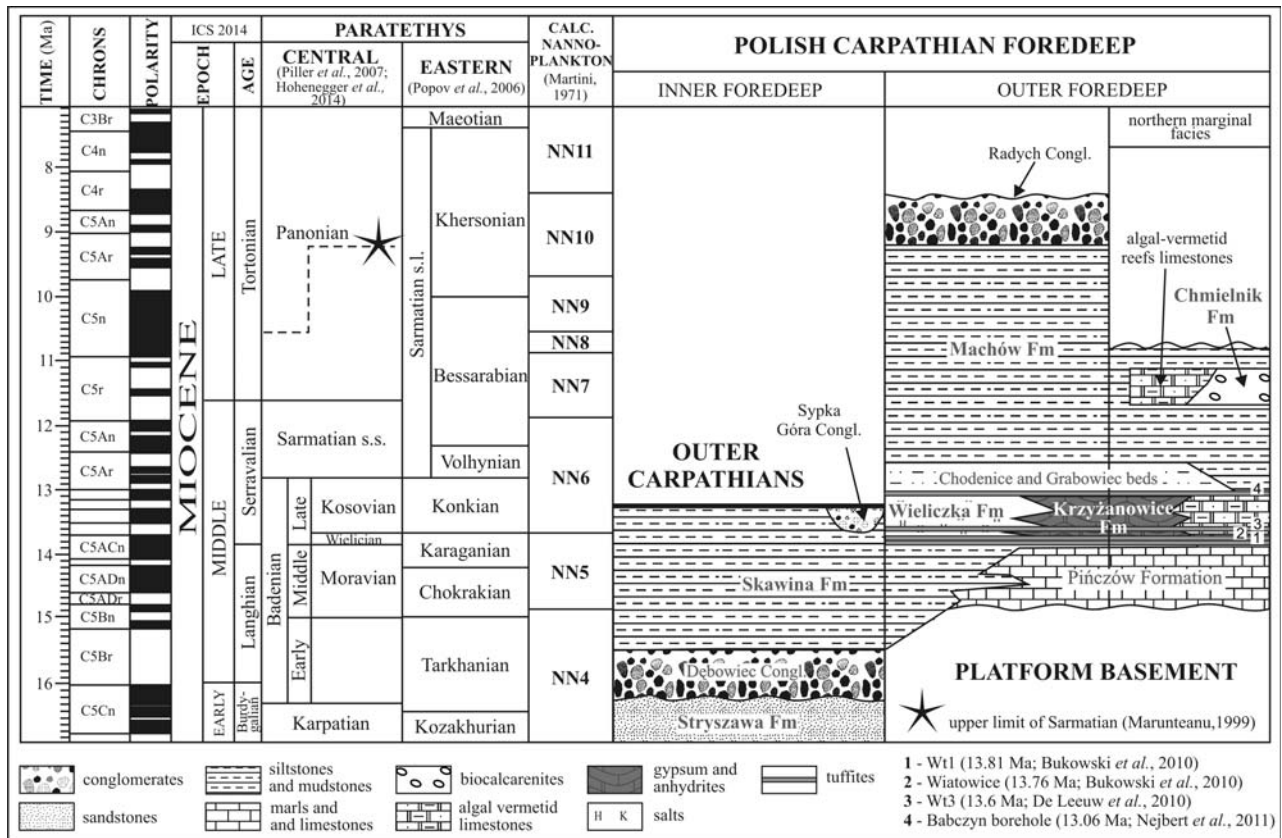


Fig. 2. Stratigraphic scheme of the Miocene deposits of the Polish Carpathian Foredeep Basin (after Oszczytko, 1998; Oszczytko *et al.*, 2006; Oszczytko and Oszczytko-Clowes, 2012, modified). Age of Badenian-Sarmatian boundary after Hohenegger *et al.* (2014).

According to geophysics and well data, the platform basement with a Miocene molasse cover dips southwards beneath the Outer Carpathian nappes to a distance of at least 50 km (Oszczytko and Ślęczka, 1985; Oszczytko, 2006).

The PCFB can be subdivided into inner and outer sub-basins, situated respectively south and north of the Carpathian frontal thrust. The former, beneath the Carpathian nappes, is composed of Early to Middle Miocene autochthonous and allochthonous deposits, the thickness of which is up to 1500 m. The latter is filled with the Middle Miocene (Badenian and Sarmatian) autochthonous strata, reaching a thickness of a few hundred metres in the northern marginal part and up to 3500 m in the south-eastern part (Oszczytko *et al.*, 2006). The Early Miocene deposits are mostly terrestrial in origin, whereas the Middle Miocene strata are marine and associated with the extensive early Badenian transgression, which flooded both the foredeep and marginal part of the Carpathians (Oszczytko *et al.*, 2006; Oszczytko and Oszczytko-Clowes, 2012). Figure 2 presents the stratigraphic scheme of the outer foredeep, the subject matter of the present work, and to some extent that of the inner part.

BIO- AND CHRONOSTATIGRAPHY OF THE BADENIAN AND SARMATIAN DEPOSITS OF THE PCFB

The Badenian strata in the outer part of the PCFB traditionally were subdivided into 3 lithostratigraphic units: the

lower Badenian sub-evaporitic, the middle-Badenian evaporitic and the upper-Badenian supra-evaporitic units (Ney, 1968; Ney *et al.*, 1974). According to the recent Early–Middle Miocene integrated stratigraphy of the Central Paratethys (Piller *et al.*, 2007; Hohenegger *et al.*, 2009, 2011, 2014), the Badenian stage is divided as follows: early Badenian (16.303–15.032 Ma), middle Badenian (Moravian: 15.032–13.82 Ma) and late Badenian (Wielician: 13.82–13.65 Ma; Kosovian: 13.65–12.829 Ma). The Badenian-Sarmatian boundary is dated at 12.829 Ma.

The sub-evaporitic unit in the north-eastern part of the PCFB is represented by the Pińczów Formation, which is the equivalent of the Skawina Formation in the western part (Jasionowski and Peryt, 2004; Oszczytko *et al.*, 2006). According to determinations of calcareous nannoplankton, the lower part of this formation belongs to the NN5 Zone, while its upper (sub-salt) part is referable to the NN6 Zone (Gaździcka, 1994; Garecka *et al.*, 1996; Andreyeva-Grigorovich *et al.*, 1997, 2003; Peryt, 1999; Peryt and Gedl, 2010).

The evaporitic unit (Wieliczka and Krzyżanowice formations), the major correlative horizon in the PCFB (Peryt, 2006, and references therein; see also Garecka and Olszewska, 2011), belongs to the lower part of the NN6 Zone, corresponding to the late Badenian (Peryt, 1997; Peryt *et al.*, 1997, 1998; Andreyeva-Grigorovich *et al.*, 2003, 2008; Peryt and Gedl, 2010).

The evaporites are covered by late Badenian (Kosovian) and Sarmatian deposits (Gaździcka, 1994; Andreyeva-Grigorovich *et al.*, 1999; Olszewska, 1999; Andreyeva-

Grigorovich *et al.*, 2003). In the Kraków–Bochnia area, the salt deposits are overlain by clays and mudstones of the Chodenice Beds, which pass upwards into the Grabowiec Beds (Porębski and Oszczytko, 1999; see also Andreyeva-Grigorovich *et al.*, 2003). To the north, the thickness of the Chodenice Beds decreases to a few dozen metres, to be replaced by marly claystones of the *Spirialis/Pecten* beds. The *Pecten* Beds occur along the northern part of the PCFB and pass towards the SE into open marine deposits of the *Spirialis* Beds (Jurkiewicz and Karnkowski, 1961). East of the Dunajec River, the evaporites are covered by the thick clayey-sandy deposits of the Machów Formation, reaching 1500 m in thickness in the central part and 2500 m in the eastern part (Alexandrowicz *et al.*, 1982; Oszczytko *et al.*, 2006), the so-called Krakovets (Krakowiec) Shale or Krakovets Beds (Łomnicki, 1897, Ney *et al.*, 1974; Piwocki *et al.*, 1996). As a facies unit, the Krakovets Shale is subdivided on the basis of fossils into the *Syndesmya (Abra)* Beds in the lower part and the *Serpula-Ctenophora* Beds above (Pawłowski *et al.*, 1985).

Gaździcka (1994) assigned the *Pecten* and overlying *Syndesmya* beds to the undivided NN8–NN9 zones. Within the *Pecten* Beds, associated with the post-evaporite Kosovian transgression and marine deposition, a rhyolite tuffite layer was dated (Ar/Ar) to give an average age of 13.06 ± 0.11 Ma (Nejbert *et al.*, 2010; Śliwiński *et al.*, 2012). This indicates that the *Pecten* Beds were deposited during the lower part of the NN6 Zone, not during the NN8 Zone or later, as was formerly suggested (Gaździcka, 1994), whereas the Badenian–Sarmatian transition in the PCFB took place soon after 13.06 ± 0.11 Ma (Nejbert *et al.*, 2010; Śliwiński *et al.*, 2012). Furthermore, in the PCFB the Badenian salinity crisis ended before *ca.* 13.06 ± 0.11 Ma (Nejbert *et al.*, 2010; Śliwiński *et al.*, 2012), which is consistent with other radiometric results, according to which the crisis began shortly after 13.81 ± 0.08 Ma and the deposition of evaporites took place *ca.* 13.60 ± 0.07 Ma (De Leuw *et al.*, 2010). Thus both the evaporites and the *Pecten* Beds represent the lower part of the NN6 Zone.

In 1966, Odrzywolska-Bieńkowska identified the *Anomalinoidea dividens* and *Elphidium hauerinum* zones in the Krakovets Beds (Łuczowska, 1964) and pointed out the limitations on foraminiferal age assignments for the Late Miocene, both in the Mediterranean and Paratethys areas (Odrzywolska-Bieńkowska, 1966; see also Olszewska, 1999).

Jurkiewicz (in: Ney, 1969) in turn identified two Sarmatian foraminiferal zones with *Anomalinoidea dividens* and *Quinqueloculina* sp. in the Krakovets Beds. In further studies of these deposits, Odrzywolska-Bieńkowska (1972) and Łuczowska (1972) described foraminiferal zones, representing the early and middle Sarmatian (Volhynian–Besarabian).

For the Krakovets Beds in the northeastern part of the PCFB, Gaździcka (1994) suggested the NN8 *Catinaster coalithus* Zone or even the NN9 *Discoaster hamatus* Zone (Sarmatian, according to Gaździcka, 1994; Pannonian, according to Piller *et al.*, 2007; see also Garecka and Olszewska, 2011).

Subsequent studies on the foraminiferal associations (Czepiec, 1997; Olszewska, 1999) indicated the late Badenian–late Sarmatian age of the Krakovets Beds (the early

Sarmatian *Anomalinoidea dividens* horizon and the lower part of the late Sarmatian *Protelphidium subgranosum* horizon). Olszewska (1999) considered the calcareous nannofossil to be more diagnostic for the Late Miocene deposits, by comparison with the foraminifera.

Garecka and Jugowiec (1999) assigned the Machów Formation (the *Pecten* Beds and the Krakovets Shale) to the NN5 (Kupno area) and NN6 (Cegielnica and Dębica areas) zones (early Badenian).

Paruch-Kulczycka (1999) assigned the upper part of the Krakovets Beds to the Pannonian (early Late Miocene), on the basis of thecamoebians and foraminifera.

Extensive studies of the Machów Formation were carried out in the Sokołów-Smolarzyny area in the eastern part of the PCFB, north of Rzeszów (Krzywiec *et al.*, 2008; see also Oszczytko-Clowes *et al.*, 2012). Calcareous nannofossil data were evidence of the NN6 Zone in the lower part of the Machów Formation and the NN7 Zone in the upper part (Oszczytko-Clowes in: Krzywiec *et al.*, 2008).

In 2011, Garecka and Olszewska presented results from the Middle Miocene deposits in SE Poland and Western Ukraine, which confirmed the reliability of the foraminiferal zones described by Łuczowska (1964) and the high degree of correlation between the Polish and Ukrainian assemblages (the *Pecten/Spirialis* beds and the Kosiv Formation, respectively). The supra-evaporitic deposits were assigned to the calcareous nannoplankton NN6, NN6–NN7 and NN7 zones. Calcareous nannofossils assemblages, observed both in the Polish and Ukrainian part of the Carpathian Foredeep (the Krakovets Beds and the upper part of the Kosiv and Dashava formations), were also similar, so that correlation based on this group also was possible (Garecka and Olszewska, 2011).

MATERIAL AND METHODS

Presented studies of the Machów Formation were concentrated in the eastern part of the Polish Carpathian Foredeep Basin (PCFB) in the Sieniawa–Rudka area, within the Miocene Ryszkowa Wola Horst (Fig. 1). A total of 55 samples were collected from two boreholes at the following depth intervals (depth in regard to ground level): Rudka-13 (28 samples): 520–538 m, 550–538 m, 558–569 m; Wylewa-1 (27 samples): 660–678 m, 820–838 m.

Slides were prepared using the simple smear-slide technique (Bown and Young, 1998). The slides were examined under the light microscope (LM) Nikon Eclipse E600 POL under cross-polarized and transmitted light at x1000 magnification. The simple smear-slide preparation technique was used for relative abundance count analyses. Results of these analyses and further statistical treatment are presented in Tables 1–6 and Appendix Tables 1 and 2.

In each sample, the relative abundance of individual nannofossil taxa was determined by counting up to 300 specimens per slide. According to Thierstein *et al.* (1977, *vide* Bown and Young, 1998), at the 95% confidence level 300 specimen counts ensure the presence of a taxon, the relative abundance of which was 1% of the total population. In the majority of samples, the number of specimens greatly exce-

eded 300. After reaching the required number of coccoliths, a further 200 fields of view were checked for biostratigraphically and palaeoecologically significant, but rarer species.

The individual numbers of specimens of autochthonous taxa and species found, but not previously counted (marked as “x”), were listed in Tables 5 and 6 and used as input data in complex statistical analysis. Following Ćorić and Švábenická (2004), these species were grouped into “Miocene *s.s.* taxa” and “taxa with their last occurrence mentioned during the Miocene”. The former expression concerns species with their first occurrence known from the Miocene. The latter includes long-ranging taxa, which occur in the Palaeogene and extend into the Miocene; hence the specimens of these species can be autochthonous or reworked from older strata. The third group distinguished as clearly “allochthonous taxa” was excluded from the statistical analysis. This group includes reworked species of Early Miocene, Palaeogene (mostly Eocene) and Cretaceous age. For the purpose of age assignment, several biostratigraphic schemes were applied in this paper, namely zonations proposed by Martini and Worsley (1970), Bukry and Okada (1980), Theodoridis (1984), Fornaciari *et al.* (1996) and Young (1998). Periodical palaeogeographic changes have reflected the size of coccoliths through the time, thus in the case of some species the morphometry is also taken as a stratigraphic criterion, e.g. *Coccolithus miopelagicus* (> 14 µm).

For estimation of the numerical proportion of an individual taxon in a sample, the following formula was used:

$$p = \frac{x}{n}$$

where x is a number of specimens counted and n is a fixed total number of specimens of all species (in this case 300). Assuming the random character of the counts, according to Drooger (1978), the statistical error in p may be considered to be equal to the theoretical standard deviation, thus the proportion of a taxon in the statistical population can be given as:

$$p \pm \sqrt{\frac{p \cdot (1-p)}{n}}$$

(multiplied by 100 to obtain percentages; Appendix Tabs 1, 2). For the purpose of the present study, only the quantitative data for autochthonous assemblages are discussed in detail, although some of the long-ranging taxa may have been reworked from older strata. On the basis of relative abundance, the percentages of autochthonous and clearly allochthonous components were estimated, taking into account the fixed total of 300 specimens with a statistical error calculated according to the formula given above. Sample data were investigated using multivariate cluster analysis of a matrix of Euclidean distance measures between species, performed by Ward's method (Ward, 1963), with subsequent determination of the species, indicative of the clusters obtained (Dufrêne and Legendre's indicator value method, 1997). Ward's method uses an analysis-of-variance approach to evaluate the distances between clusters. In brief, it attempts to reduce the sum of squares of any two (hypothetical) clusters that can be formed at each step (Hammer *et al.*, 2001, *vide* Watkins, 2007). According to Dufrêne and Legendre (1997), the indicator value index (*INDVAL*) is de-

Table 1

Distribution of autochthonous calcareous nannofossils in the Rudka-13 and Wylewa-1 boreholes

Species	RUDKA-13 (28)		WYLEWA-1 (27)	
	Specimens	Samples	Specimens	Samples
<i>Braarudosphaera bigelowii</i>	39	15	136	27
<i>Calcidiscus macintyreii</i>	62	20	40	10
<i>Calcidiscus premacintyreii</i>	1	1	1	1
<i>Coccolithus miopelagicus</i> (> 14 µm)	167	28	100	25
<i>Coccolithus pelagicus</i>	959	28	872	27
<i>Coronocyclus nitescens</i>	62	23	96	27
<i>Cyclicargolithus floridanus</i>	647	28	810	27
<i>Discoaster deflandrei</i>	12	10	14	11
<i>Discoaster exilis</i>			1	1
<i>Helicosphaera carteri</i>	118	28	87	26
<i>Helicosphaera intermedia</i>	30	18	38	23
<i>Helicosphaera walbersdorfensis</i>	23	14	26	13
<i>Pontosphaera discopora</i>	37	21	24	16
<i>Pontosphaera multipora</i>	195	28	189	27
<i>Reticulofenestra haggii</i>	106	27	95	23
<i>Reticulofenestra pseudoumbilica</i> (> 7 µm)	654	28	746	27
<i>Reticulofenestra minuta</i>	243	27	357	27
<i>Sphenolithus abies</i>	44	20	58	20
<i>Sphenolithus moriformis</i>	220	28	217	27
<i>Umbilicosphaera rotula</i>	2	2	7	5

defined as follows: for each species j in each cluster of sites k , one computes the product of two values, A_{kj} , a measure of specificity based on abundance values, and B_{kj} , a measure of fidelity, computed from presence data:

$$A_{kj} = N_{individuals_{kj}} / N_{individuals_{+k}}$$

$$B_{kj} = N_{sites_{kj}} / N_{sites_{+k}}$$

$$INDVAL_{kj} = A_{kj} \times B_{kj} \times 100$$

In the first formula, $N_{individuals_{kj}}$ is the mean abundance of species j across the sites pertaining to cluster k . $N_{individuals_{+k}}$ is the sum of the mean abundances of species j within the various clusters. Using the mean number of individuals in each cluster, instead of summing the individuals across all sites of clusters, removes any effect of variations in the number of sites belonging to the various clusters (Dufrêne and Legendre, 1997; Legendre, 2013). A_{kj} reaches a maximum, when species j is present only in cluster k . In the formula for B_{kj} , $N_{sites_{kj}}$ is the number of sites in cluster k where species j is present and $N_{sites_{+k}}$ is the total number of sites in that cluster. B_{kj} is a maximum, when species j is present at all sites of cluster k . The quantities A and B represent the independent features of species distribution; hence, they must be combined by multiplication. A final multiplication by 100 gives percentages. $INDVAL_{kj}$ reaches a maximum (= 100%), when the individuals of species j are observed in all sites, belonging to a single cluster. $INDVAL_j = \max[INDVAL_{kj}]$ means that of species $INDVAL_j$ for a partition of sites is the largest value of $INDVAL_{kj}$ noted over all clusters k of that partition (Dufrêne and Legendre, 1997).

Table 2

Distribution of allochthonous calcareous nannofossils in the Rudka-13 and Wylewa-1 boreholes

Species	RUDKA-13 (28)		WYLEWA-1 (27)	
	Specimens	Samples	Specimens	Samples
<i>Blackites spinosus</i>	3	3	12	7
<i>Calcidiscus leptoporus</i>			1	1
<i>Chiasmolithus altus</i>	5	4		
<i>Chiasmolithus bidens</i>	15	10	20	16
<i>Chiasmolithus expansus</i>	12	9	15	12
<i>Chiasmolithus gigas</i>	1	1	4	4
<i>Chiasmolithus grandis</i>	10	8	13	10
<i>Chiasmolithus medius</i>	1	1	5	3
<i>Chiasmolithus modestus</i>	35	18	28	20
<i>Chiasmolithus oamaruensis</i>	11	8	24	14
<i>Chiasmolithus solitus</i>	16	11	21	16
<i>Cyclicargolithus abisectus</i>	26	17	42	17
<i>Cyclicargolithus luminis</i>	6	4	6	5
<i>Dictyococcites bisectus</i>	271	28	146	27
<i>Dictyococcites scrippsae</i>	948	28	847	27
<i>Discoaster barbadiensis</i>	25	17	24	15
<i>Discoaster binodosus</i>	7	5	3	3
<i>Discoaster lodoensis</i>	2	2	1	1
<i>Discoaster multiradiatus</i>	3	3	6	4
<i>Discoaster saipanensis</i>	5	5	7	7
<i>Discoaster sp.</i>	9	9	3	3
<i>Discoaster tanii</i>			2	2
<i>Discoaster tanii nodifer</i>	3	3	5	5
<i>Elipsolithus macellus</i>			1	1
<i>Elipsolithus distichus</i>			2	2
<i>Ericsonia fenestrata</i>	21	10	51	22
<i>Ericsonia formosa</i>	380	28	330	27
<i>Ericsonia robusta</i>	28	15	20	17
<i>Ericsonia subdisticha</i>	55	23	33	16
<i>Helicosphaera ampliapertura</i>	5	5	8	7
<i>Helicosphaera bramlettei</i>	34	15	34	21
<i>Helicosphaera compacta</i>	21	15	29	19
<i>Helicosphaera euphratis</i>	13	12	17	14
<i>Helicosphaera gartneri</i>	3	3	16	14
<i>Helicosphaera heezenii</i>			1	1
<i>Helicosphaera lophota</i>			1	1
<i>Helicosphaera mediterranea</i>	2	2	6	6
<i>Helicosphaera recta</i>	23	14	14	12
<i>Helicosphaera reticulata</i>	4	4		
<i>Helicosphaera scissura</i>	15	13	22	18
<i>Heliolithus kleinpelli</i>	4	4	7	6
<i>Isthmolithus recurvus</i>	48	23	61	26
<i>Lanternithus minutus</i>	192	27	211	27
<i>Neococcolithes dubius</i>	6	5	8	7
<i>Pontosphaera latelliptica</i>	388	28	360	27
<i>Pontosphaera plana</i>	7	4	10	9
<i>Pontosphaera rothi</i>	13	8	25	16
<i>Reticulofenestra daviesii</i>	245	28	307	27
<i>Reticulofenestra dictyoda</i>	315	27	96	27
<i>Reticulofenestra hillae</i>	116	28	98	25

Species	RUDKA-13 (28)		WYLEWA-1 (27)	
	Specimens	Samples	Specimens	Samples
<i>Reticulofenestra lockerii</i>	13	5	63	20
<i>Reticulofenestra ornata</i>			2	2
<i>Reticulofenestra reticulata</i>	287	28	245	27
<i>Reticulofenestra umbilica</i>	312	28	117	25
<i>Semihololithus kerabyi</i>	3	2	4	4
<i>Sphenolithus belemnus</i>			1	1
<i>Sphenolithus calyculus</i>			1	1
<i>Sphenolithus capricornutus</i>			1	1
<i>Sphenolithus conicus</i>	63	22	66	26
<i>Sphenolithus disbelemnus</i>	2	2	4	3
<i>Sphenolithus dissilimis</i>	6	5	8	6
<i>Sphenolithus editus</i>	14	13	31	17
<i>Sphenolithus heteromorphus</i>	7	7	11	9
<i>Sphenolithus obtusus</i>			1	1
<i>Sphenolithus predistensus</i>	1	1		
<i>Sphenolithus radians</i>	10	10	15	13
<i>Sphenolithus strigosus</i>	1	1	2	2
<i>Toweius callosus</i>	14	8	15	14
<i>Toweius emimens</i>	12	9	21	15
<i>Toweius rotundus</i>	18	13	16	13
<i>Transersopontis fibula</i>	5	4	7	5
<i>Transersopontis obliquipons</i>	15	8	37	23
<i>Transversopontis pulcher</i>	54	22	45	20
<i>Transversopontis pulcheroides</i>	24	17	29	20
<i>Tribrachiatus orthostylus</i>	3	3	2	2
<i>Zygrhablithus bijugatus</i>	202	28	201	27
Cretaceous species undivided	361	28	238	27

Table 3

Indicator values (%) of species for clusters obtained by Ward's method in the Rudka-13 borehole (highest IV bolded)

RUDKA-13	Cluster 1	Cluster 2	Cluster 3
	3 sites	10 sites	15 sites
<i>Braarudosphaera bigelowii</i>	38.76	12.21	9.3
<i>Calcidiscus macintyreii</i>	15.87	19.29	32.86
<i>Calcidiscus premacintyreii</i>	33.33	0	0
<i>Coccolithus miopelagicus (> 14 µm)</i>	45.38	28.69	25.93
<i>Coccolithus pelagicus</i>	23.8	35.38	32.66
<i>Coronocyclus nitescens</i>	53.85	24.92	14.77
<i>Cyclicargolithus floridanus</i>	29.53	38.09	32.38
<i>Discoaster deflandrei</i>	9.26	13.33	12.96
<i>Helicosphaera carteri</i>	29.33	40.8	29.87
<i>Helicosphaera intermedia</i>	29.76	22.5	12.38
<i>Helicosphaera walbersdorfensis</i>	26.32	7.11	22.11
<i>Pontosphaera discopora</i>	13.07	24.71	36.08
<i>Pontosphaera multipora</i>	46.58	27.95	25.48
<i>Reticulofenestra haggii</i>	51.22	21.95	25.04
<i>Reticulofenestra minuta</i>	34.84	28.26	2.46
<i>Reticulofenestra pseudoumbilica (> 7 µm)</i>	29.37	43.63	27
<i>Sphenolithus abies</i>	46.51	27.91	11.16
<i>Sphenolithus moriformis</i>	31.42	44.26	24.32
<i>Umbilicosphaera rotula</i>	25.64	2.31	0

Table 4

Indicator values (%) of species for clusters obtained by Ward's method in the Wylewa-1 borehole (highest IV bolded)

WYLEWA-1	Cluster 1	Cluster 2	Cluster 3	Cluster 4	Cluster 5
	3 sites	1 sites	10 sites	7 sites	6 sites
<i>Braarudosphaera bigelowii</i>	36.44	32	6.67	5.33	19.56
<i>Calcidiscus macintyreii</i>	40.28	0	6.28	0.25	11.08
<i>Calcidiscus premacintyreii</i>	0	0	0	14.29	0
<i>Coccolithus miopelagicus</i> (> 14 µm)	5.96	23.84	23.36	16.17	24.83
<i>Coccolithus pelagicus</i>	22.98	16.44	19.41	24.93	16.23
<i>Coronocyclus nitescens</i>	17.57	26.35	18.44	16.56	21.08
<i>Cyclicargolithus floridanus</i>	25.41	8.55	17.81	24.83	23.39
<i>Discoaster deflandrei</i>	10.56	0	16.63	15.51	1.32
<i>Discoaster exilis</i>	0	0	10	0	0
<i>Helicosphaera carteri</i>	13.69	20.54	28.96	10.76	22.82
<i>Helicosphaera intermedia</i>	18.37	0	29.76	15	27.56
<i>Helicosphaera walbersdorffensis</i>	4.36	52.3	3.14	4	11.62
<i>Pontosphaera discopora</i>	5.05	22.73	10.23	16.23	12.63
<i>Pontosphaera multipora</i>	19.27	12.85	26.98	21.1	19.8
<i>Reticulofenestra haqii</i>	23.72	0	19.78	13.07	27.2
<i>Reticulofenestra minuta</i>	27.85	27.85	15.32	13.38	15.61
<i>Reticulofenestra pseudoumbilica</i> (> 7 µm)	18.32	5.07	21.65	24.65	30.3
<i>Sphenolithus abies</i>	0	52.88	18.13	10.17	10.49
<i>Sphenolithus moriformis</i>	9.29	34.84	20.21	25.22	10.45
<i>Umbilicosphaera rotula</i>	12.86	0	1.74	10.63	3.21

In order to show the relations between samples and species in low-dimensional space, Nonmetrical Multidimensional Scaling (nMDS) also was used, based on Euclidean distances. All statistical analyses were performed using the STATISTICA 10 (StatSoft) software package.

RESULTS

Core material

In 2012, the authors profiled and sampled for calcareous nannoplankton studies core material from the boreholes Rudka-13 (520–538 m, 550–538 m, 558–569 m, altogether 34 boxes); Wylewa-1 (660–678 m, 820–838 m, altogether 31 boxes). Although the profiles are characterized by monotonous lithology, the subtle lithological differences are distinguishable on the curves on wells logging graphs (Krzywiec *et al.*, 2005; Mastalerz *et al.*, 2006). On the basis of 3-D seismic data and geophysical well logs, the siliciclastic series of the Machów Fm succession has been reliably correlated and subdivided into several genetic stratigraphic sequences *sensu* Galloway (1989; Krzywiec *et al.*, 2005; Mastalerz *et al.*, 2006; Fig. 3). The Miocene succession is characterized by a shallowing-upward trend of sedimentation. It consists of offshore hemipelagic, turbiditic and deltaic and nearshore-to-estuarine facies associations (Krzywiec *et al.*, 2005). Lithological logs and photographs of core material are presented on Figs 4–8.

Nannoplankton analysis

The calcareous nannofossils collected from the Rudka-13 (R-13) and Wylewa-1 (W-1) boreholes were generally abundant and well preserved. Some taxa had a medium degree of preservation or were poorly preserved in the form of smaller fragments or with broken elements, which made identification inconclusive, especially within the *Discoaster* group. Traces of dissolution were not recorded. The majority of samples were characterized by a high number of allochthonous specimens (Figs 9, 10). The estimated statistical error for autochthonous and allochthonous groups was between 2.8 and 2.9%, rounded to 3%. In the sample descriptions, the abbreviations were used. The number of sample (s.) comes from number of sampled box. Roman numbers indicate metre of depth intervals, from which samples were collected (Tabs 5, 6).

In the R-13 borehole (Fig. 9), reworked specimens generally prevail over the autochthonous specimens. In three samples (R-13 s. 26, R-13 s. 14, R-13 s. 12), their percentages are similar with a difference of only a few percent.

In the W-1 borehole (Fig. 10), the percentages of autochthonous and clearly allochthonous component are diverse. In a few samples, the occurrence of former is slightly higher, in one sample reaching a maximum value of 58.0 ± 3%. In three samples (W-1 s. 14, W-1 s. 6, W-1 s. 4), the percentages of allochthonous species are visibly higher. In the remainder of the profile, the reworked component is usually predominant or the percentages are comparable.

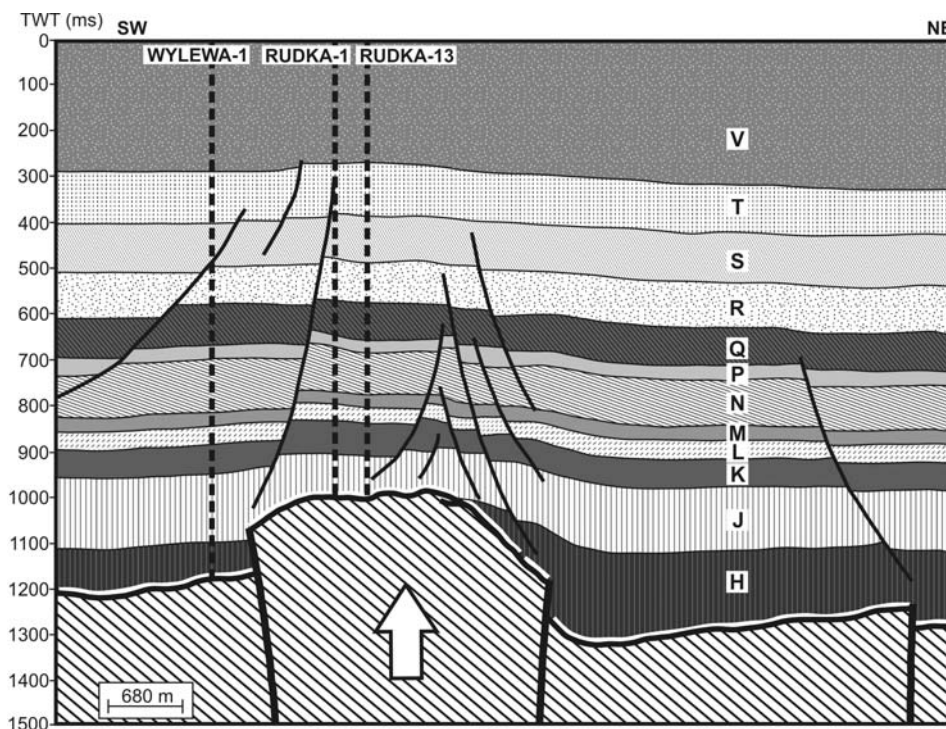


Fig. 3. Interpreted seismic profile calibrated by Wylewa-1, Rudka-1 and Rudka-13 wells. White horizon – Badenian evaporates. Genetic sequences: H, J, K – turbiditic; L, M, N – deltaic; P, Q, R, S – deltaic; T, V – low-energy nearshore to estuarine facies (after Mastalerz *et al.*, 2006, simplified). For location see Fig. 1.

The diversity of the autochthonous assemblage was low, in comparison to the allochthonous component. Within the former group, 20 species were recognized in the R-13 borehole and 21 species in the W-1 borehole, whereas within the reworked group 70 species were identified in the R-13 borehole and 76 species in the W-1 borehole, excluding the Cretaceous species that were combined in one group. The distribution of autochthonous and reworked calcareous nannofossils in R-13 and W-1 is arranged alphabetically and listed in Tabs 1 and 2.

Calcareous nannoplankton distribution

The Miocene associations from both of the boreholes investigated were dominated by the long-ranging *Coccolithus pelagicus*, *Cyclicargolithus floridanus* and *Reticulofenestra pseudoumbilica* ($> 7 \mu\text{m}$) occurring in each sample.

In the **R-13** borehole (Appendix Table 1), the abundance of *C. pelagicus* varies between $7.0 \pm 1.5\%$ and $15.0 \pm 2.1\%$, but usually is higher than 11%. The occurrence of *C. floridanus* is relatively lower and in the majority of samples its percentage is between $5.7 \pm 1.3\%$ and $9.3 \pm 1.7\%$, usually under or around 8%. Another prevailing species is *R. pseudoumbilica* ($> 7 \mu\text{m}$) with a variable percentage oscillating between $2.7 \pm 0.9\%$ and $12.3 \pm 1.9\%$. Only a few samples reach values of above 10%. Relatively less commonly recorded were specimens of *Reticulofenestra minuta*, *Sphenolithus moriformis*, *Pontosphaera multipora* and *Coccolithus miopelagicus* ($> 14 \mu\text{m}$). *Helicosphaera carteri* is present in each sample with its occurrence often under or around 2%. *Reticulofenestra haqii* occurs with variable abundance. With lower and irregular frequency, species such as

Calcidiscus macintyreii, *Coronocyclus nitescens*, *Sphenolithus abies* and *Braarudosphaera bigelowii* were noted. Specimens of *Pontosphaera discopora*, *Helicosphaera intermedia* and *Helicosphaera walbersdorfensis* occurred irregularly, at under or just above 1%. Among the rare discoasterids, only *Discoaster deflandrei* and *Discoaster exilis* were observed. Specimens of *Calcidiscus premacintyreii* and *Umbilicosphaera rotula* and *Rhabdosphaera procera* rarely occurred.

In the **W-1** borehole (Appendix Table 2), the abundance of *C. pelagicus* varies between $5.3 \pm 1.3\%$ and $14.7 \pm 2.0\%$. In the majority of samples, it occurs in amounts above or just below 10%, higher than *R. minuta*. The abundance of *C. floridanus* in most samples is also relatively high, at above or around 10%. The occurrence of *R. pseudoumbilica* ($> 7 \mu\text{m}$) was mostly between $6.3 \pm 1.4\%$ and $14.7 \pm 2.0\%$ with a maximum in sample W-1 s. 7. Such species as *Reticulofenestra minuta*, *Sphenolithus moriformis* and *Pontosphaera multipora* occur relatively less frequently but regularly. *Braarudosphaera bigelowii* was present in each sample with a variable frequency, but higher up in the profile (interval 660–678 m), the values slightly increase and reach a maximum in sample W-1 s. 3. *C. miopelagicus* ($> 14 \mu\text{m}$) occurs irregularly. Specimens of *C. nitescens* were observed continuously with a frequency from $0.3 \pm 0.3\%$ to $3.0 \pm 1.0\%$. *Reticulofenestra haqii* was present in the majority of samples, amounting to mainly below or just around 2%. *Helicosphaera carteri* occurs continuously, with an abundance of usually under or just above 1%. Specimens of *Sphenolithus abies*, *Calcidiscus macintyreii*, *Heli-*

Table 5

Autochthonous calcareous nannofossil assemblages from the Rudka-13 borehole

	AUTOCHTHONOUS																		SUMMARY	ALLOCHTHONOUS			
	Miocene s.s. taxa													Taxa with their last occurrence during the Miocene									
RUDKA-13	<i>Calcidiscus macintyrei</i>	<i>Calcidiscus premacintyreii</i>	<i>Coccolithus miopelagicus</i> (> 14 µm)	<i>Coronocyclus nitescens</i>	<i>Discoaster exilis</i>	<i>Helicosphaera carteri</i>	<i>Helicosphaera intermedia</i>	<i>Helicosphaera walbersdorfensis</i>	<i>Reticulofenestra haggii</i>	<i>Reticulofenestra haggii</i>	<i>Reticulofenestra pseudumbilica</i> (> 7 µm)	<i>Rhabdosphaera procera</i>	<i>Sphenolithus abie</i>	<i>Umbilicosphaera rotula</i>	<i>Braarudosphaera bigelowii</i>	<i>Coccolithus pelagicus</i>	<i>Cyclicargolithus floridanus</i>	<i>Discoaster deflandrei</i>	<i>Pontosphaera discopora</i>	<i>Pontosphaera multipora</i>	<i>Sphenolithus moriformis</i>		
520-538 I s. 1			8	2		1	2	1	5	11	23		4		6	23	25	x	1	10	9	131	169
520-538 II s. 2	x		10	3		5		2	8	13	8		2		x	33	36	x	2	5	6	133	167
520-538 III s. 3	1		5	5		10	x	x	3	10	27		5	x	x	38	27	1	2	4	14	152	148
520-538 IV s. 4	2		15	2		5	x	2	8	9	22		1		4	21	17	1	1	13	6	129	171
520-538 V s. 5	1		10	1		1	1		1	5	28		2		2	37	20	x	2	3	13	127	173
520-538 VI s. 6	2	1	5	10		5	3		8	7	17		3	1	x	22	18		x	11	8	121	179
520-538 VII s. 7	3		4			6			4	7	15		3		1	39	18		1	10	9	120	180
520-538 VIII s. 8			10	3		1	1	2	6	12	21		2		2	33	19	2	x	11	1	126	174
520-538 IX s. 9	1		4	3		5	x	x	1	6	26		1	x	2	35	20	x	3	5	15	127	173
520-538 X s. 10			1	1		2	3		3	9	33		2		1	35	31		1	11	9	142	158
520-538 XI s. 11	1		3	2		2	3	4	1	7	28		1			34	17	2	1	9	5	120	180
520-538 XII s. 12	1		1	5		9	1	1	2	7	33		3	1		36	28		x	9	9	146	154
520-538 XIII s. 13			1	2		1	1	1	1	7	20		1		1	35	21		2	8	5	107	193
520-538 XIV s. 14	1		12	1		4	x		7	16	23					45	25	x	1	4	8	147	153
520-538 XV s. 15			4	1		6			5		19		x			43	35	1	3	11	7	135	165
520-538 XVI s. 16	1		8	x		5	1		2	3	28		x		4	33	26	1	1	6	14	133	167
520-538 XVII s. 17			2	1		7	1		3	2	19				2	36	24	1	3	5	5	111	189
520-538 XVIII s. 18			6	1		7	1		5	10	19		1		x	39	21	x	2	5	5	122	178
550-558 I s. 19	1		11	4		5	x	1	5	9	36	x	x		x	25	22	1	2	8	5	135	165
550-558 V s. 23	1		10	x		3	2		2	6	37		5		x	28	26	x	x	11	8	139	161
558-569 I s. 25	2		3	1		2	1		3	8	25		x		1	35	21		2	4	6	114	186
558-569 II s. 26	4		5	3	x	5	1	4	7	10	31		1		5	31	32	1	x	6	3	149	151
558-569 III s. 27	2		2	2		2	1	1	3	22	22		1		3	38	14	1	2	5	5	126	174
558-569 V s. 29	15		6	5		3	x	1		10	18				x	44	22			4	8	136	164
558-569 VI s. 30	1	x	4	2		6	3	x	4	8	28		1		x	29	26	x	1	5	18	136	164
558-569 VII s. 31	4		6	2		3	4	1	2	10	15				2	33	21		3	3	4	113	187
558-569 VIII s. 32	12		1			6		1	2	11	13		1			42	17			5	9	120	180
558-569 IX s. 33	6		10	x		1	x	1	5	8	20		4		3	37	18		1	4	6	124	176

(x – species found, not counted)

cosphaera intermedia, *H. walbersdorfensis* and *Pontosphaera discopora* were recorded less commonly and irregularly. Scarce specimens of *Discoaster deflandrei*, *Umbilicosphaera rotula*, *Calcidiscus premacintyreii* and *Discoaster exilis* were also observed.

In the **Rudka-13** and **Wylewa-1** boreholes, the clearly allochthonous component (Table 2) was mainly composed of *Dictyococcites scrippsae*, *Pontosphaera latelliptica*, *Erico-*

nia formosa and species of Late Cretaceous age. Such species as *Reticulofenestra dictyoda*, *R. umbilica*, *R. reticulata*, *R. daviesii*, *R. hillae*, *Dictyococcites bisectus*, *Zygrhablithus bijugatus* and *Lanternithus minutus* also occur commonly.

Multivariate analysis

In the **Rudka-13** borehole, cluster analysis by Ward's method differentiated 3 main clusters (Figs 11, 12). Cluster

Table 6

Autochthonous calcareous nannofossil assemblages from the Wylewa-1 borehole

	AUTOCHTHONOUS TAXA																	SUMMARY	ALLOCHTHONOUS TAXA			
	Miocene s.s. taxa											Taxa with their last occurrence during the Miocene										
WYLEWA-1	<i>Calcidiscus macintyreii</i>	<i>Calcidiscus premacintyreii</i>	<i>Coccolithus miopelagicus</i> (> 14 µm)	<i>Coronocycclus nitescens</i>	<i>Discoaster exilis</i>	<i>Helicosphaera carteri</i>	<i>Helicosphaera intermedia</i>	<i>Helicosphaera walbersdorffensis</i>	<i>Reticulofenestra haqii</i>	<i>Reticulofenestra minuta</i>	<i>Reticulofenestra pseudoumbilica</i> (> 7 µm)	<i>Sphenolithus abies</i>	<i>Umbilicosphaera rotula</i>	<i>Braarudosphaera bigelowii</i>	<i>Coccolithus pelagicus</i>	<i>Cyclicargolithus floridanus</i>	<i>Discoaster deflandrei</i>	<i>Pontosphaera discopora</i>	<i>Pontosphaera multipora</i>	<i>Sphenolithus moriformis</i>		
660-678 I s. 1			1	5		1	1	3		20	25		2	6	38	31	2	2	5	5	147	153
660-678 III s. 3	6		1	3		1	1	x	11	23	21		x	25	34	39	x		6	3	174	126
660-678 IV s. 4			4	5		3		4		22	6	7		12	26	12		1	4	15	121	179
660-678 VI s. 6			5	9		1	1	2	3	12	28	1	2	3	16	33	x	1	4	6	127	173
660-678 VII s. 7	7		2	5		3	1	2	5	16	44	2		7	26	38			1	3	162	138
660-678 VIII s. 8			5	3		2	2	1	6	8	30	2		6	21	39	1	1	7	9	143	157
660-678 X s. 10	2		1	1		10	1	3	7	18	37	3		12	25	30	x	x	8	2	160	140
660-678 XI s. 11				6		4	2	1	9	20	27	3	x	1	32	31			7	8	151	149
660-678 XII s. 12	2		5	3		3	1		4	14	39			9	31	28	x	1	6	4	150	150
660-678 XIII s. 13	9		1	2		4	1		6	23	19			10	37	37	x		7	4	160	140
660-678 XIV s. 14	5		7	3		4	1	1	2	7	24			4	30	22			6	11	127	173
660-678 XV s. 15	6			4		7	x		5	12	25	3		1	29	34	2	x	7	7	142	158
660-678 XVI s. 16			1	2		4	1		5	15	22		1	1	43	37		x	6	5	143	157
820-838 I s. 17			6	4	1	x	2		4	10	26	3		3	33	28	1	1	4	7	133	167
820-838 II s. 18			9	2		8	3	2	5	8	22			9	31	21	x		13	5	138	162
820-838 III s. 19			4	2		1		3	2	14	30	2		3	41	35	1	2	7	16	163	137
820-838 IV s. 20		1	4	5		1	1	x		6	34	1	1	2	33	29	1	1	6	11	137	163
820-838 V s. 21	1		1	5		2	2	2	1	18	22	5		1	30	26	1	2	7	9	135	165
820-838 VI s. 22	1		8	3		6	2		2	13	29	6		3	20	21	1	3	8	6	132	168
820-838 VIII s. 24	1		3	1		1	1	1	2	10	27	1		1	42	34	1	2	8	11	147	153
820-838 IX s. 25			6	6		7	2		3	6	22	4		1	37	25	2	2	7	13	143	157
820-838 X s. 26			2	2		1	x		3	11	20	2		4	44	35	1	1	7	11	144	156
820-838 XI s. 27			7	1		5	2			12	31	2		1	31	17		x	11	12	132	168
820-838 XII s. 28			2	5		1	1	1	4	10	36	2		2	38	39	x	1	6	6	154	146
820-838 XIII s. 29			5	1		4	2		4	15	28	4		1	34	25		1	14	9	147	153
820-838 XIV s. 30			7	3		1	3		1	6	37	2		7	35	29		2	11	3	147	153
820-838 XV s. 31			3	5		2	4	x	1	8	35	3	1	1	35	35	x		6	16	155	145

(x – species found, not counted)

1 is characterized by the presence of all characteristic species and high indicator values (IV) from 9.26 to 53.85% (bolded values, Table 3) This cluster groups 3 samples, situated in the upper part of the profile. On the nMDS plot, this group appears to be distinctive from the other one, situated on the left side of the first axis and the lower part of the second axis. In Cluster 2, *Calcidiscus premacintyreii* is absent. Samples belonging to this cluster on the nMDS plot are located from the centre to the left side of the first axis and from the centre of the second axis to its upper part. In Clus-

ter 3 *Calcidiscus premacintyreii* and *Umbilicosphaera rotula* are absent. Only two species have high indicator values, namely *Pontosphaera discopora* and *Calcidiscus macintyreii*. Samples of Cluster 3 are positioned in nMDS from the centre of first axis to the right part of the first axis and in the second axis from the centre to its upper part. In the centre of the nMDS plot, Cluster 2 and Cluster 3 make contact.

In the **Wylewa-1** borehole, 5 clusters were differentiated (Figs 13, 14). The main indicator species are shown in Table 4 (bolded values). In Cluster 1, *Calcidiscus prema-*

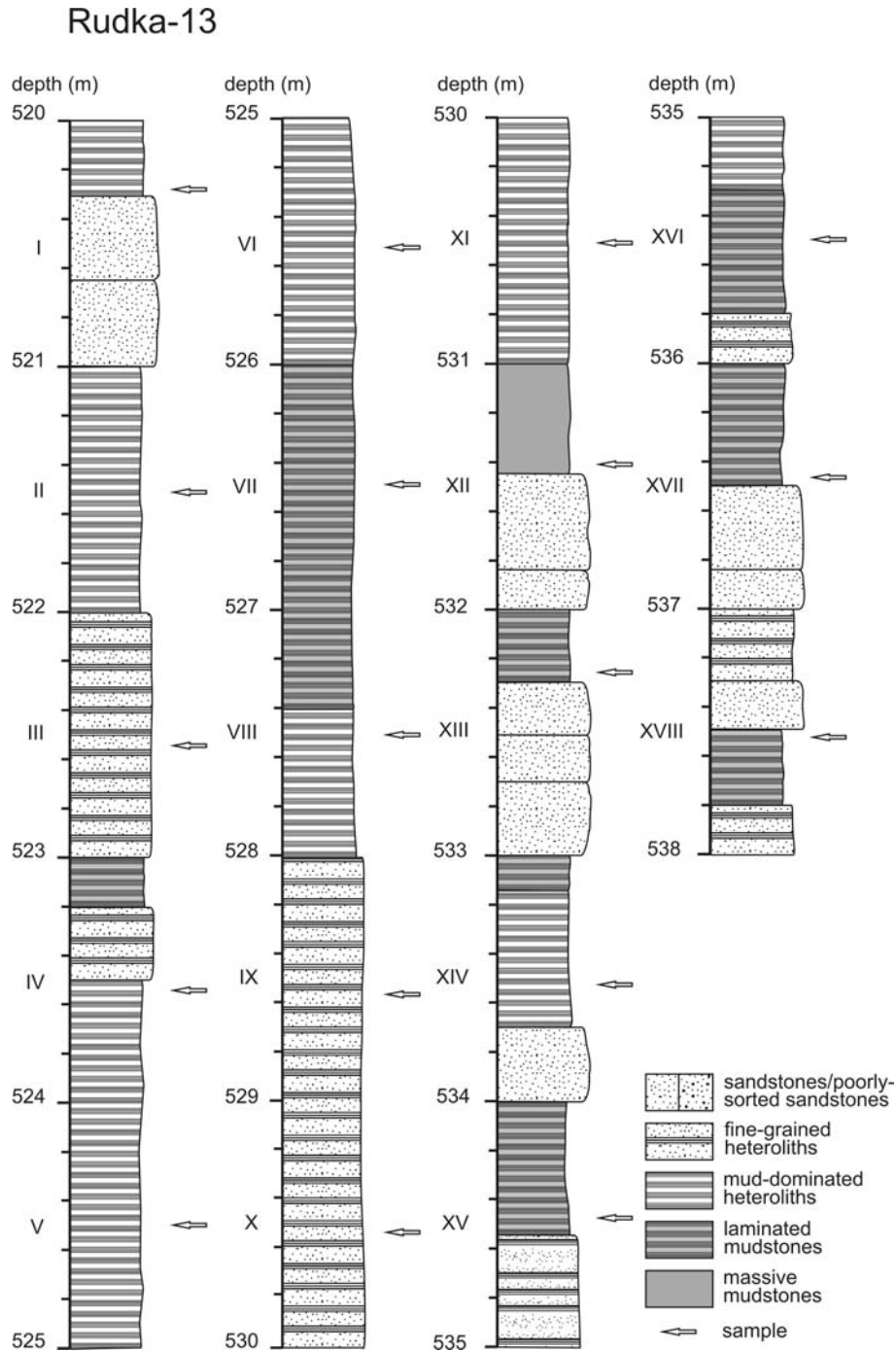


Fig. 4. Lithological log of core material from the Rudka-13 borehole (520–538 m).

cintyreii, *Discoaster exilis* and *Sphenolithus abies* are absent. In the nMDS plot, species belonging to this cluster are located in the centre of the first axis and in the upper part of the second axis, intermingling with Cluster 4. In Cluster 2, a lot of species are absent, namely *Calcidiscus macintyreii*, *Calcidiscus premacintyreii*, *Discoaster deflandrei*, *Discoaster exilis*, *Helicosphaera intermedia*, *Reticulofenestra haqii* and *Umbilicosphaera rotula*. This cluster represents only one sample, located in the right part of the first axis and close to the centre of the second one. In Cluster 3, only *Calcidiscus premacintyreii* is absent. On the nMDS plot, samples are situated from the centre of the first axis to the

right and from the centre of the second axis to its lower part. In Cluster 4, all species can be found, except for *Discoaster exilis*. Samples of Cluster 3 in nMDS are positioned around the centre of the first axis and from the centre to the upper part of the second axis, making tangential contact with Cluster 4. In Cluster 5, *Calcidiscus premacintyreii* and *Discoaster exilis* are absent. On nMDS, samples are located from the centre of the first axis to the left and from the centre of the second axis to its lower part.

The sequence of clusters along the core is shown in Figure 9 and Figure 10 on the right axis. In the R-13 borehole, samples alternate mostly between Cluster 2 and 3 through-

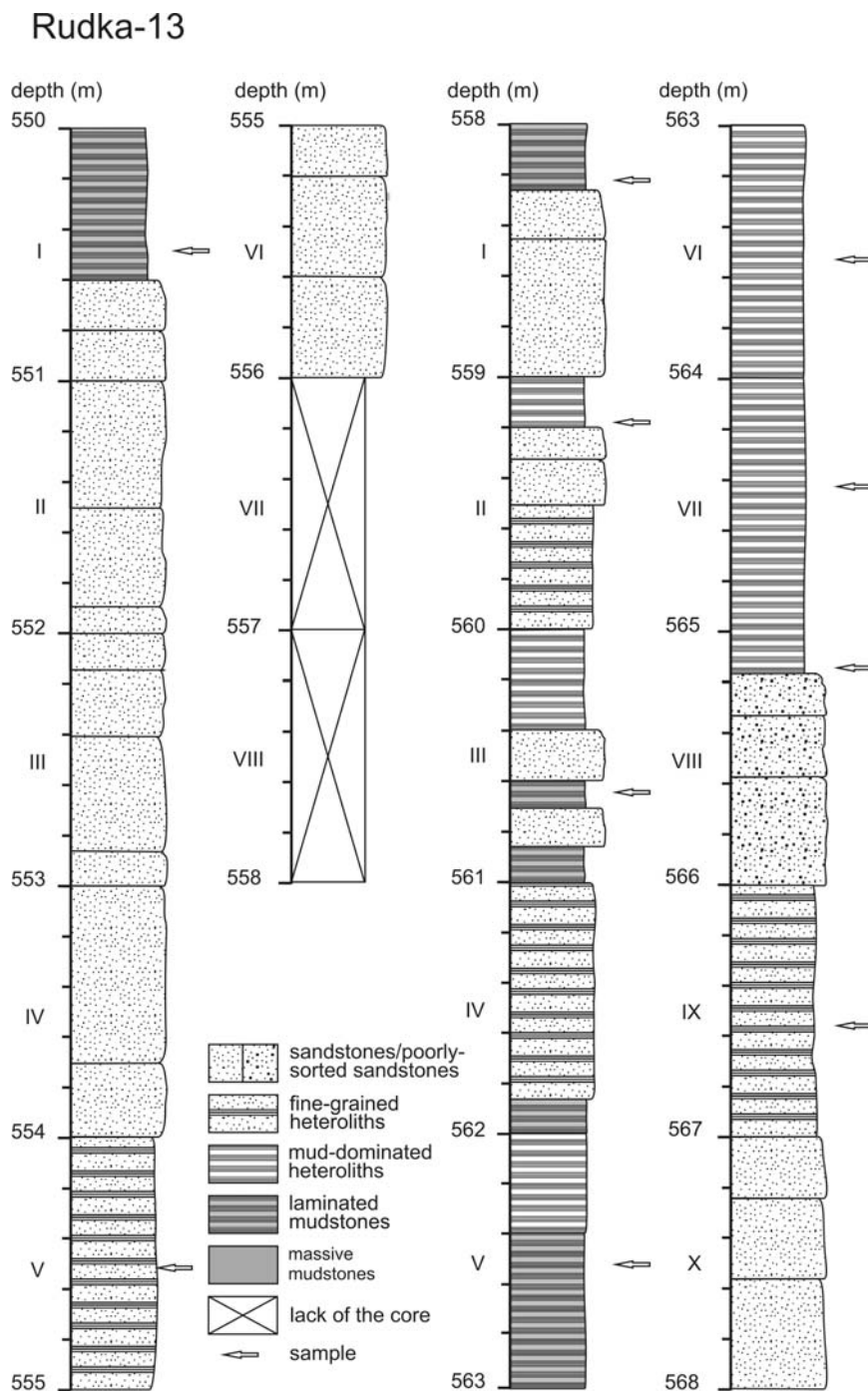


Fig. 5. Lithological log of core material from the Rudka-13 borehole (550–568 m).

out the entire profile. Three samples belonging to Cluster 1 are situated in the upper part and strongly alternate with Cluster 2 and 3. In W-1, samples belonging to Cluster 1 are situated in the uppermost part of the profile and one sample a few metres lower. Cluster 2 represents only one sample, located in the upper part of the profile. Samples of Cluster 3 and Cluster 4 alternate with each other in the interval 820–830 m and in the lower part of the interval 660–678 m. Samples of Cluster 5 occur mostly in the upper part of the profile.

DISCUSSION

Biostratigraphy

The standard calcareous nannofossil zonation of the Miocene was constructed mainly on the basis of first (FO) or last occurrence (LO) of *Discoaster* species, the distribution of which was presumably controlled ecologically and depended on palaeogeography. Discoasters occur much more often in the Mediterranean area than in the Paratethys (Perch-Nielsen, 1985). Therefore the Miocene zonations of Martini and Worsley (1970) and Bukry and Okada (1980) usually are readily obtained in lower latitudes, where

Wylewa-1

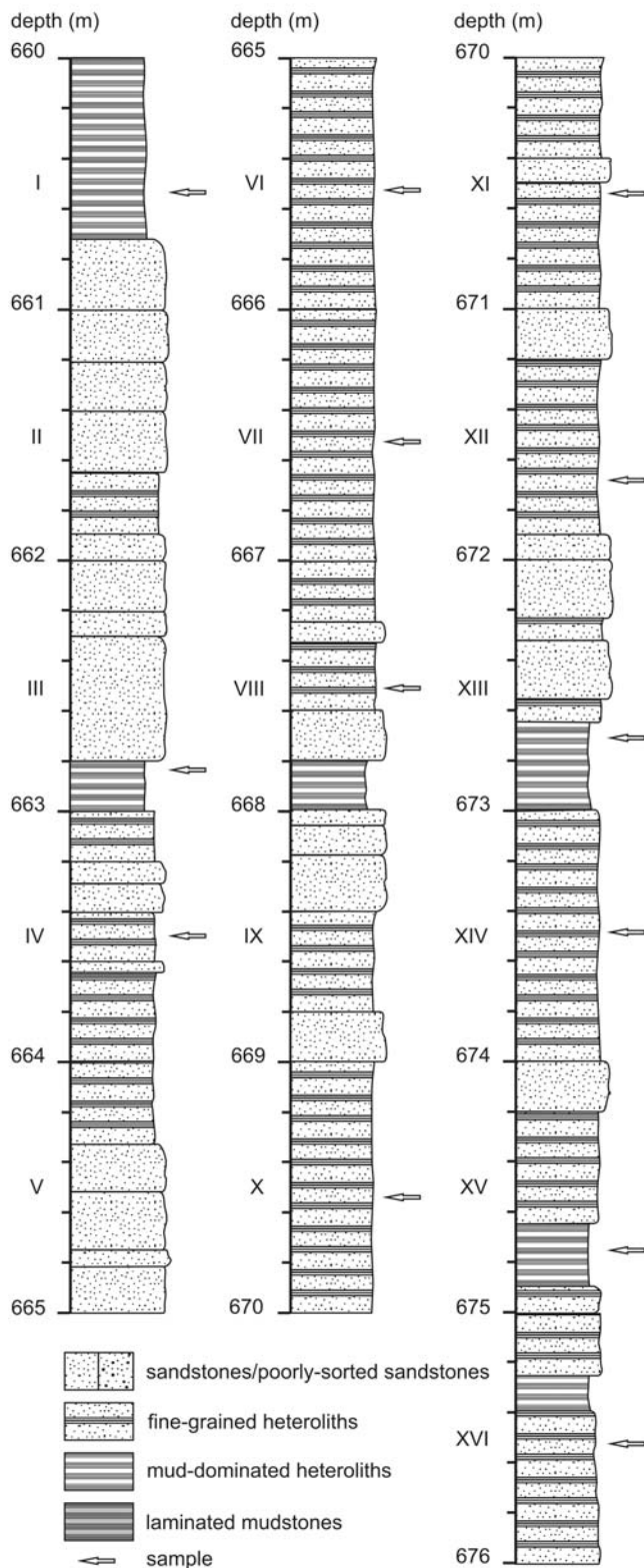


Fig. 6. Lithological log of core material from the Wylewa-1 borehole (660–676 m).

discoasters are common in open-ocean assemblages. This also applies to other index species (Perch-Nielsen, 1985). In such cases it is necessary to use alternative species for the

Wylewa-1

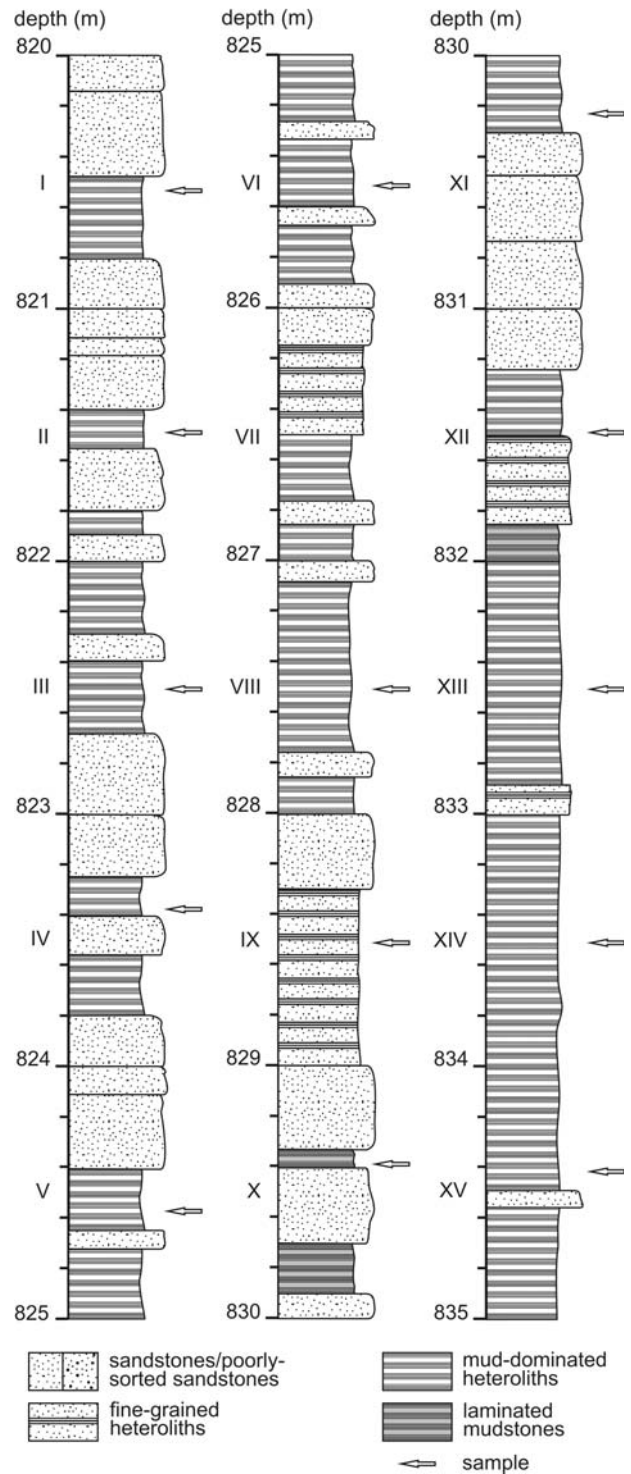


Fig. 7. Lithological log of core material from the Wylewa-1 borehole (820–835 m).

Paratethys (Perch-Nielsen, 1985). According to Báldi-Beke (1982), helicoliths are neither purely oceanic nor typical nearshore in distribution, which resulted in their expansion in the unstable palaeoenvironmental conditions of the Carpathian Foredeep and brought about an increase in their stratigraphical importance (see Švábenická, 2002).

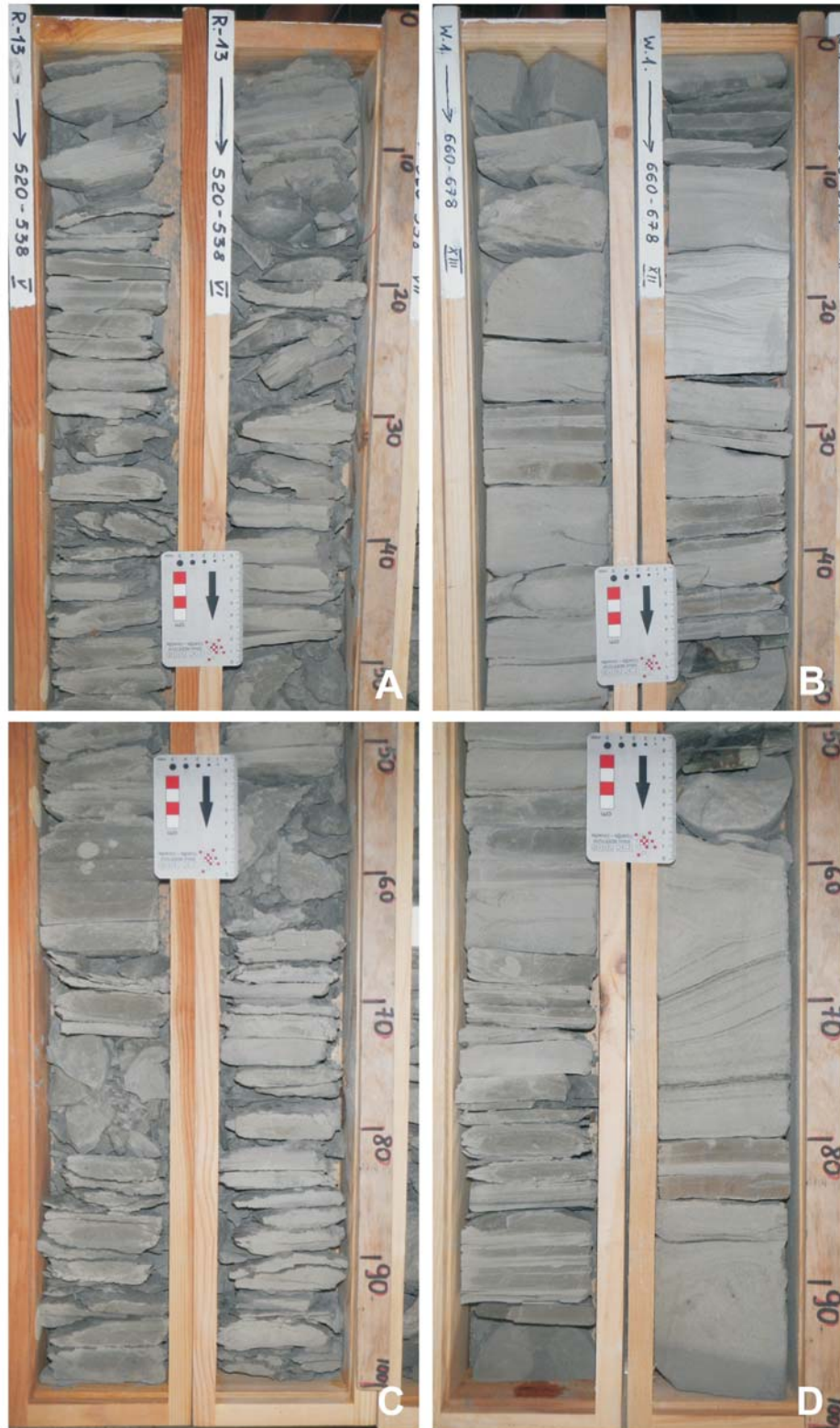


Fig. 8. Photographs of core material from the Rudka-13 and Wylewa-1 boreholes. **A, C.** Intervals: R-13 520–538 V (mud-dominated heteroliths horizontal stratified), R-13 520–538 VI (mud-dominated heteroliths, horizontal stratified). **B, D.** Intervals: W-1 660–678 XIII (fine-grained sandstones horizontal and cross-stratified, mud-dominated heteroliths horizontal stratified), 660–678 XII (fine-grained sandstones, fine-grained heteroliths horizontal and cross-stratified).

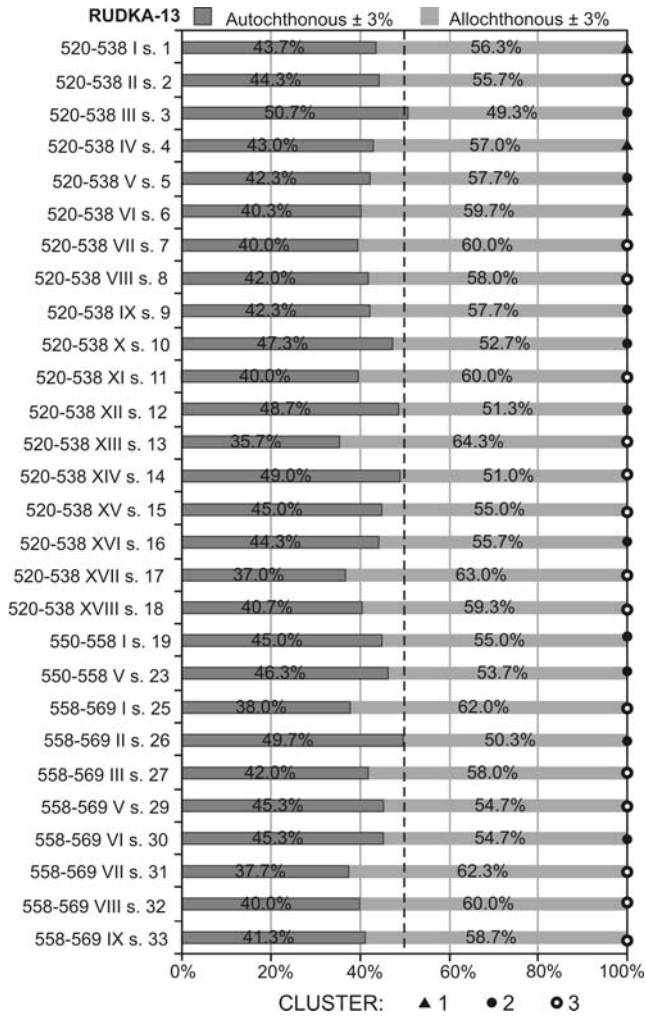


Fig. 9. Percentage abundance of autochthonous and allochthonous species in samples from the Rudka-13 borehole.

The composition of nannoplankton assemblages in the Rudka-13 and Wylewa-1 boreholes gave evidence of undivided NN6–NN7 zones. These biozones are extremely difficult to distinguish in the Central Paratethys realm, owing to the fact that in high latitudes discoasters and *C. coalithus* are scarce or absent (Bartol, 2009, and references therein). LM microphotographs of the typical Miocene calcareous nannofossils associations observed in the core samples are presented on Figs 15, 16.

The *Discoaster exilis* Zone (NN6) is defined by the last occurrence (LO) of *Sphenolithus heteromorphus* to the first occurrence (FO) of *Discoaster kugleri* and/or the LO of *Cyclicargolithus floridanus* (Hay, 1970; Martini, 1971; see also Perch-Nielsen 1985). *C. floridanus* gradually disappeared in NN6 and was replaced by abundant *Reticulofenestra pseudumbilica* (> 7 µm) near the top of this zone.

The *Discoaster kugleri* Zone (NN7) begins with the FO of *Discoaster kugleri* and/or the LO of *C. floridanus* to the FO of *Catinaster coalithus* (Bramlette and Wilcoxon, 1967; Martini, 1971; Bukry and Okada, 1980; see Perch-Nielsen, 1985). Six-rayed discoasters, such as *D. challengerii*, *D. aff. brouweri* and *D. bollii*, also occur. *C. floridanus* definitely disappears, whereas *Discoaster deflandrei* decreases

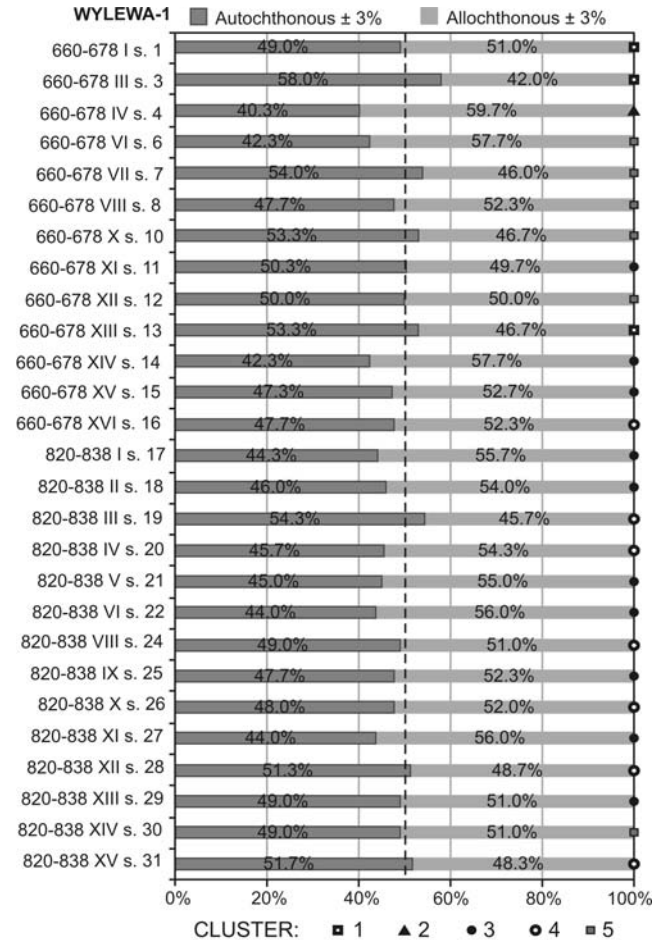


Fig. 10. Percentage abundance of autochthonous and allochthonous species in samples from the Wylewa-1 borehole.

in abundance and disappears near the top of NN7 (Perch-Nielsen, 1985). Furthermore the FO of *D. kugleri* is a problematic event, since unambiguous specimens never occur commonly. Lehotayova and Molčíková (1978, *vide* Garecka and Olszewska, 2011), owing to the absence of *D. kugleri*, assigned the upper Badenian (Kosovian substage) to the NN6 Zone. Cicha *et al.* (1998) consider that the extent of the NN6 Zone (upper Badenian–lower Sarmatian) does not allow determination of the Badenian–Sarmatian boundary exclusively on the basis of calcareous nannoplankton (see Garecka and Olszewska, 2011). Taking into account all these constraints, NN6 and NN7 were joined together (Young, 1998; see also Oszczypko-Clowes *et al.*, 2009; Garecka and Olszewska, 2011, and literature therein).

According to Young (1998), the interval NN6–NN7 is characterized by low species diversity, as lots of the taxa of earlier assemblages become less frequent or completely disappear. Therefore, a unit defined on the basis of negative criteria can be difficult to subdivide. The most common for NN6–NN7 are species, such as *Reticulofenestra pseudumbilica*, *Coccolithus pelagicus*, *Calcidiscus leptoporus*, *Discoaster exilis*, *Helicosphaera carteri*, *Umbilicosphaera jafari*, *U. rotula*. Less frequent, but biostratigraphically more

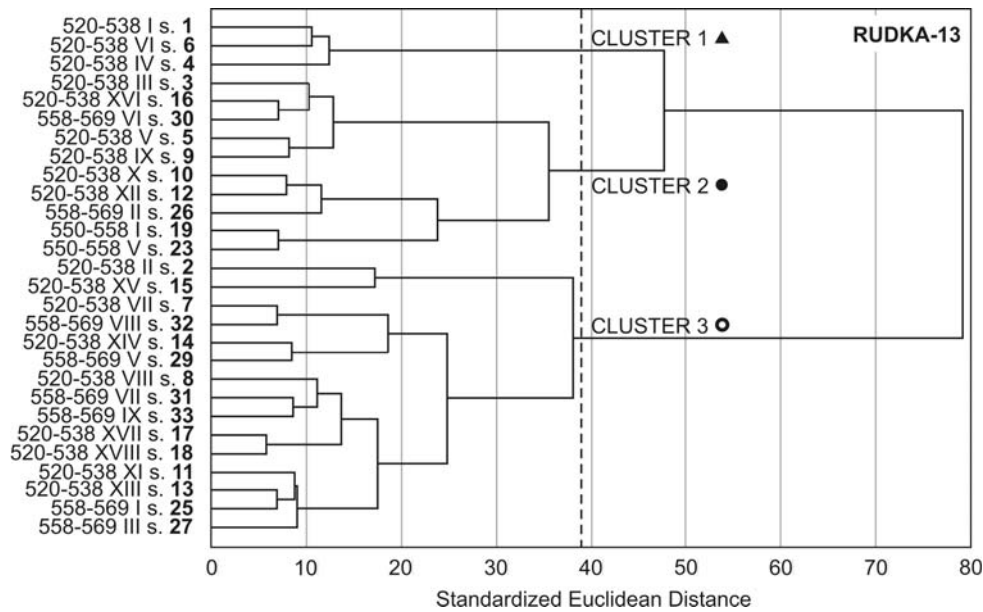


Fig. 11. Dendrogram of sample clusters resulting from Ward's method (Rudka-13).

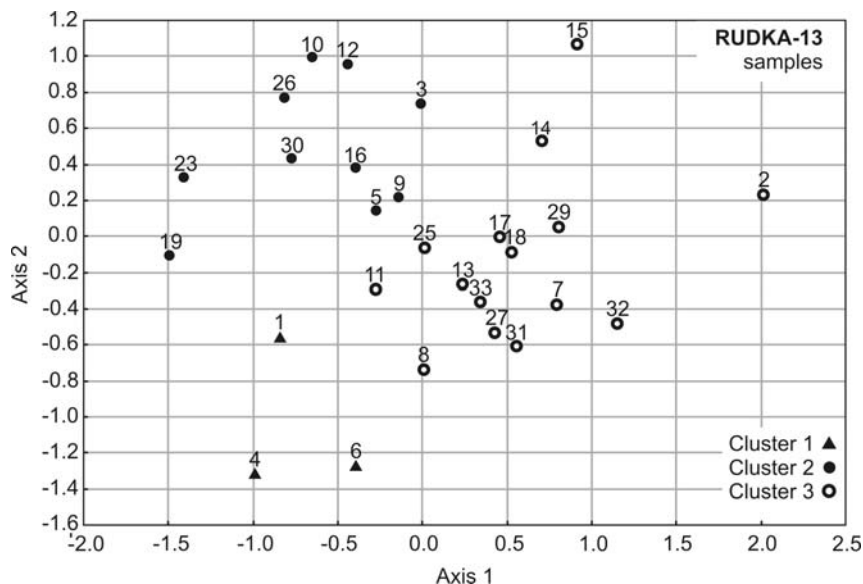


Fig. 12. Nonmetrictal Multidimensional Scaling (nMDS) of samples (Rudka-13).

useful, are *Triquetrorhabdulus rugosus*, *Discoaster kugleri* and *Helicosphaera orientalis*. The large species *Coccolithus miopelagicus* ($> 14 \mu\text{m}$) is also confined to the NN7 Zone, but its FO is gradational (Young, 1998). According to Galović and Young (2012), the large *Coccolithus miopelagicus* is a useful marker within the Sarmatian, especially its LO which is observed at the NN7-NN8 boundary in the Paratethys.

The Miocene associations from the R-13 and W-1 boreholes were dominated by *C. pelagicus*, *C. floridanus* and *R. pseudoumbilica* ($> 7 \mu\text{m}$). The first two species belong to long-ranging taxa, but there are no criteria for recognition of which specimens are redeposited. As mentioned above, the LO of *C. floridanus* was proposed by Bukry and Okada (1980) as an alternative event to the FO of *D. kugleri* for the

base of NN7, but according to Fornaciari *et al.* (1990), the LO of *C. floridanus* is diachronous in different latitudes and geographic regions and therefore must be used with caution in biostratigraphy. In mid and high latitudes, this species occurs up to the Late Miocene (Garecka and Olszewska, 2011). Galović and Young (2012) mention the LO of *C. floridanus* as being a very useful indicator of the NN6-NN7 boundary, although some overlap between *D. kugleri* and *C. floridanus* was observed (Varol, pers. comm., *vide* Galović and Young, 2012). In the equatorial Pacific, the LO of this species was dated at 13.32 Ma (Turco *et al.*, 2002), in the equatorial Atlantic at 12.65 Ma (Olafsson, 1989) and in the Mediterranean at 13.3 Ma (Hilgen *et al.*, 2003, *vide* Bartol, 2009). In the North Atlantic, a decrease in abundance of *C. floridanus* was recorded at 13.2 Ma, but scarce specimens

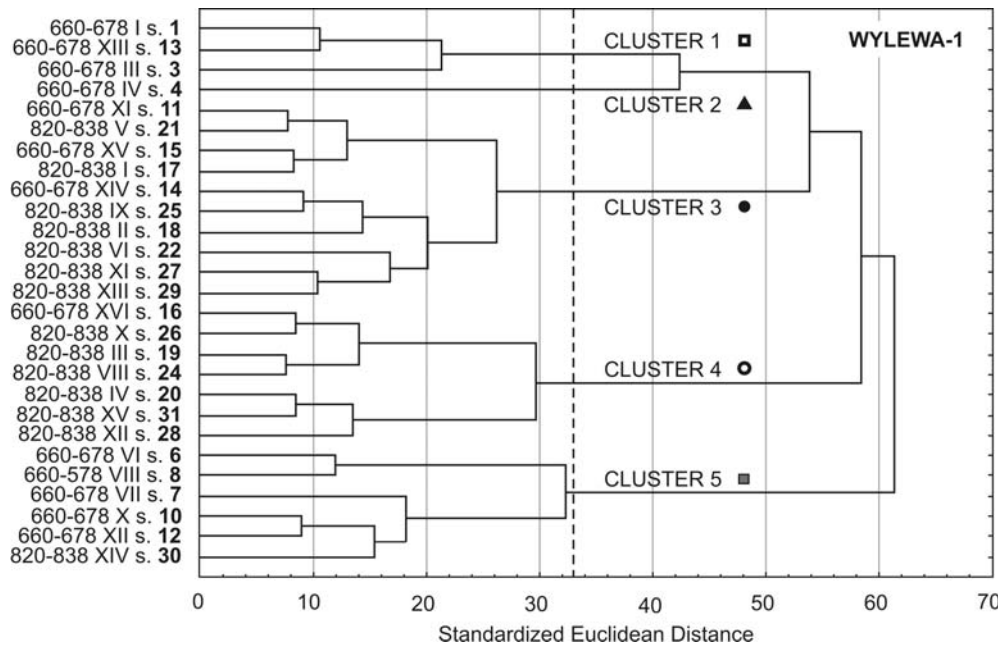


Fig. 13. Dendrogram of sample clusters resulting from Ward's method (Wylewa-1).

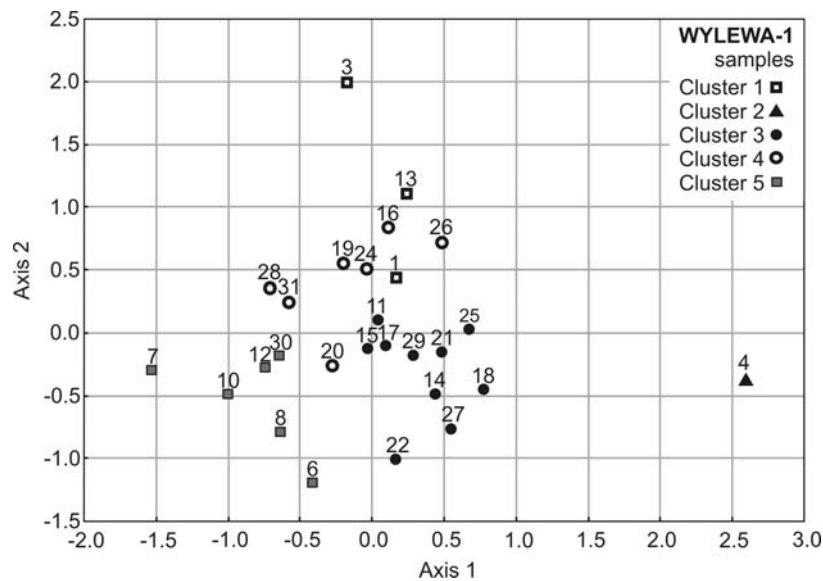


Fig. 14. Nonmetrical Multidimensional Scaling (nMDS) of samples (Wylewa-1).

were still observed at 11.9 Ma (Gartner, 1992; see Bartol, 2009). The FO of *R. pseudumbilica* ($> 7 \mu\text{m}$), takes place at the very top of NN5. This event is considered as an alternative marker for the NN5-NN6 boundary (Fornaciari *et al.*, 1990; Young, 1998). Reticulofenestrid taxonomy strongly depends on placolith size concepts and hence the differences in estimation of its FO (Fornaciari *et al.*, 1990). According to Fornaciari *et al.* (1996), the FCO of *R. pseudumbilica* ($> 7 \mu\text{m}$) can be considered as reliable in the Mediterranean record and useful to identify the sub-zonal boundary (see Bartol, 2009) between MNN6a (lower NN6) and MNN6b (upper NN6). The first common occurrence (FCO) of *R. pseudumbilica* ($> 7 \mu\text{m}$) was dated at 13.10 Ma (Abdul Aziz *et al.*, 2008). Galović and Young (2012) consider

the abundant to almost monofloral appearance of large *R. pseudumbilica* ($> 7 \mu\text{m}$) with the subsequent last occurrence or absence of *C. floridanus* as the beginning of the Sarmatian, which were observed in the Hrvatsko Zagorje Basin and in the North Croatia Basin. In the profiles studied by the present authors, *R. pseudumbilica* ($> 7 \mu\text{m}$) is one of the predominant species in the assemblages. Specimens of *Calcidiscus macintyreii* were observed much less frequently, but in the majority of samples. The contradictions in estimation of its FO are partly associated with different taxonomic concepts (Fornaciari *et al.*, 1996). In the present study, the authors consider *C. macintyreii* species equal to or larger than $11 \mu\text{m}$ (see Fornaciari *et al.*, 1996, and literature therein). According to Fornaciari *et al.* (1990), if *C. macin-*

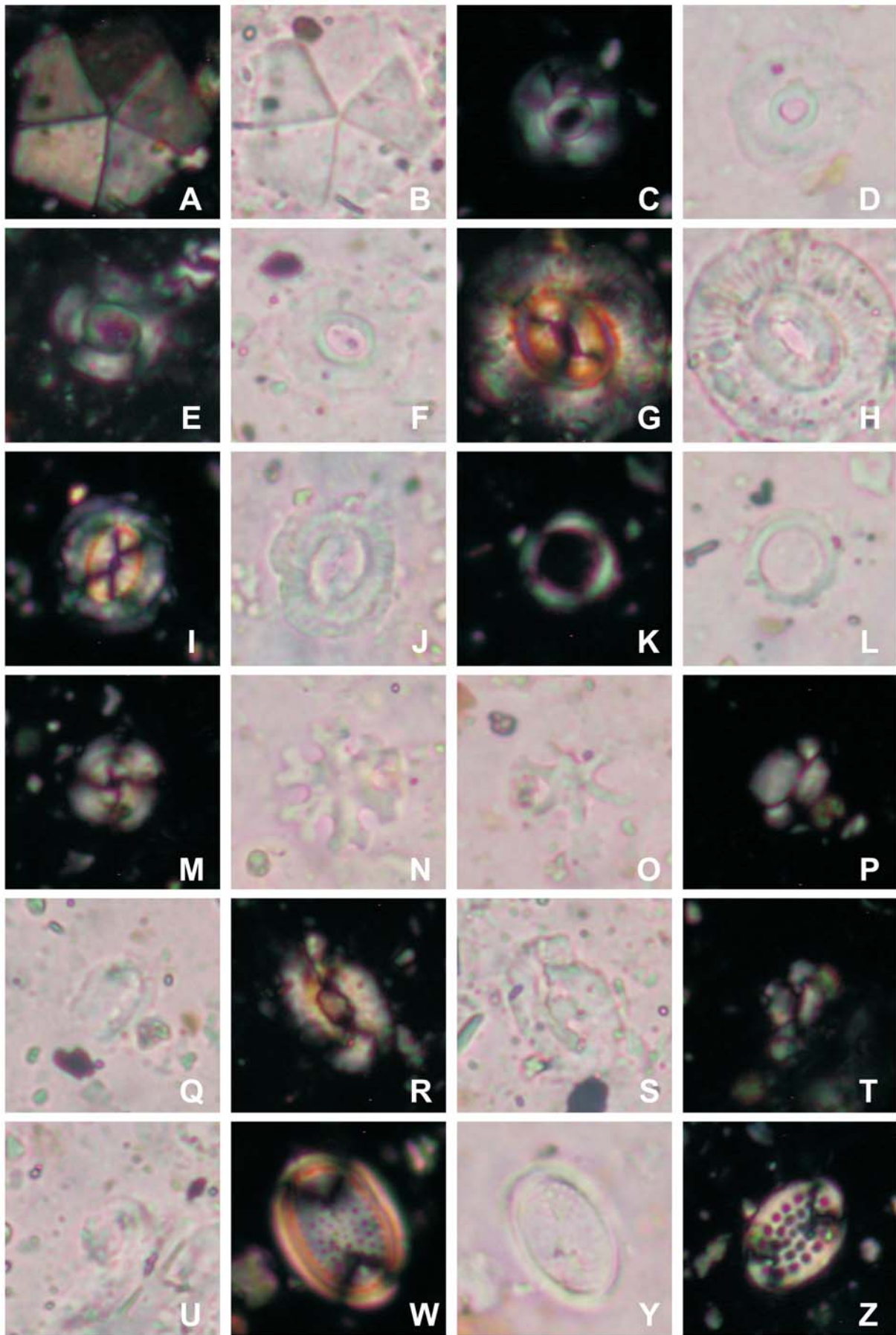


Fig. 15. LM microphotographs of the Miocene calcareous nannofossils assemblages identified in the core samples. **A, B.** *Braarudosphera bigelowii* (Gran and Braarud) Deflandre (W-1: 660–678 VI s. 6). **C, D.** *Calcidiscus macintyreii* (Bukry and Bramlette) Loeblich and Tappan (W-1: 660–678 X s. 10). **E, F.** *Calcidiscus premacintyreii* Theodoridis (R-13: 520–538 VI s. 6). **G, H.** *Coccolithus miopelagicus* (> 14 µm) Bukry (W-1: 660–678 VI s. 6). **I, J.** *Coccolithus pelagicus* (Wallich) Schiller (R-13: 520–538 IX s. 9). **K, L.** *Coronocyclus nitescens* (Kamptner) Bramlette and Wilcoxon (W-1: 820–838 XV s. 31). **M.** *Cyclicargolithus floridanus* (Roth and Hay in Hay *et al.*, 1967) Bukry (W-1: 660–678 VI s. 6). **N.** *Discoaster deflandrei* Bramlette and Riedel (R-13: 558–569 VI s. 30). **O.** *Discoaster exilis* Martini and Bramlette (W-1: 660–678 VI s. 6). **P, Q.** *Helicosphaera carteri* (Wallich) Kamptner (W-1: 660–678 XI s. 11). **R, S.** *Helicosphaera intermedia* Martini (W-1: 660–678 VI s. 6). **T, U.** *Helicosphaera walbersdorfensis* Müller (W-1: 660–678 VI s. 6). **W, Y.** *Pontosphaera discopora* Schiller (R-13: 558–569 IX s. 33). **Z.** *Pontosphaera multipora* (Kamptner ex Deflandre) Roth (R-13: 550–558 V s. 23).

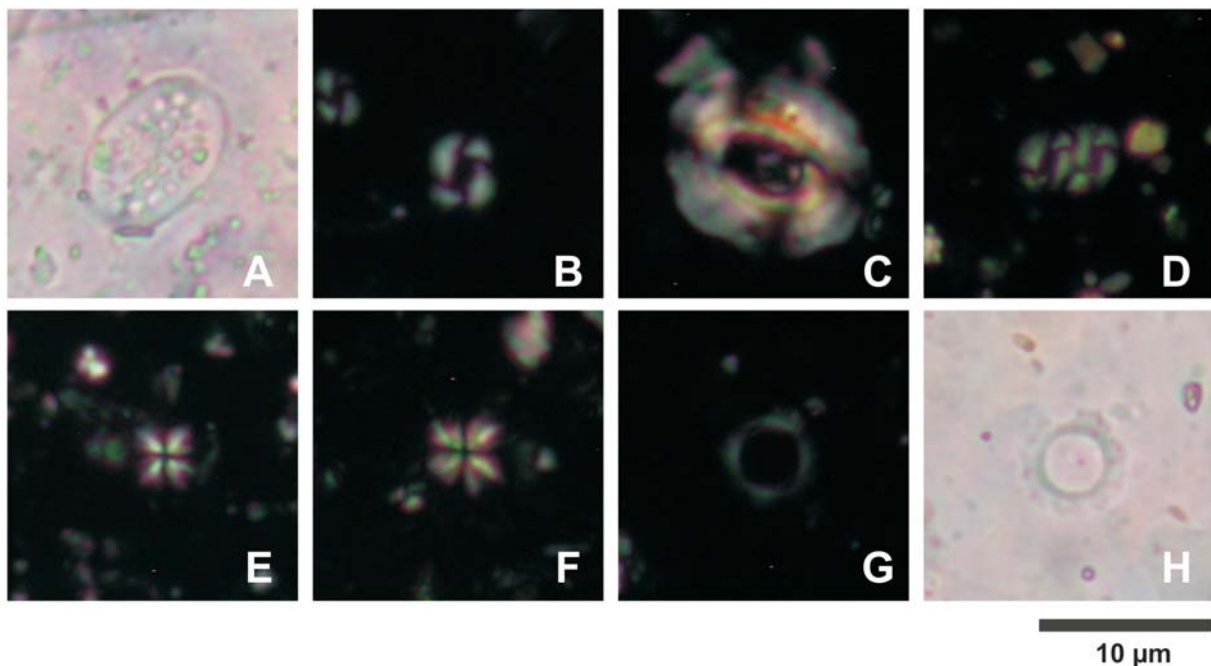


Fig. 16. LM microphotographs of the Miocene calcareous nannofossils assemblages identified in the core samples. **A.** *Pontosphaera multipora* (Kamptner ex Deflandre) Roth (R-13: 550–558 V s. 23). **B.** *Reticulofenestra haqii* Backman (W-1: 820–838 I s. 17). **C.** *Reticulofenestra pseudoubilica* (> 7 µm) (Gartner) Gartner (W-1: 660–678 VI s. 6). **D.** *Reticulofenestra minuta* Roth (W-1: 820–838 I s. 17). **E.** *Sphenolithus abies* Deflandre in Deflandre and Fert (R-13: 520–538 III s. 3). **F.** *Sphenolithus moriformis* (Brönnimann and Stradner, 1960) Bramlette and Wilcoxon (W-1: 660–678 VI s. 6). **G, H.** *Umbilicosphaera rotula* (Kamptner) Varol (R-13: 520–538 XII s. 12).

tyrei is restricted to forms of this size, its FO can be assigned to the interval between the FOs of *D. kugleri* and *C. coalithus* (NN7). Nagymarosy (1985, *vide* Garecka, 2014) describes *C. macintyreii* from the NN7 Zone assemblage (Hungary). Fornaciari *et al.* (1996) did not use the FO of *C. macintyreii* as a zonal boundary, owing to its low abundance, although Foresi *et al.* (2002) suggest that this event, if not taken as a zonal boundary marker, can be used in the Mediterranean to improve the stratigraphic resolution in the topmost part of the MMN6b Subzone (upper NN6 Zone). Švábenická (2002) and Ćorić and Švábenická (2004) describe this species from the NN6 Zone or even from the NN5 Zone. According to Peryt (1997), *C. macintyreii* occurs with *S. heteromorphus* in the NN5 assemblage, while it is found together with *D. exilis*, *H. walbersdorfensis* and small reticulofenestrads in the NN6 assemblage. The FO of *C.*

macintyreii was dated at 13.16 Ma (Turco *et al.*, 2002). Owing to the diachronous occurrence of *C. macintyreii* in different latitudes, Olafsson (1989) and Raffi and Flores (1995) do not consider its FO to be a good stratigraphic marker (see Bartol, 2009). According to Fornaciari *et al.* (1990), the LO of *C. nitescens* seems to be a better event than the FO of *D. kugleri* for the subdivision of the NN6–NN7 interval. In both profiles, single specimens of *C. nitescens* occur in almost all samples. According to Müller (1981) and Fornaciari *et al.* (1996) the LO of *Helicosphaera walbersdorfensis* can be considered as being close to the LO of *D. kugleri* and to the FO of *C. coalithus*. Müller (1981, *vide* Fornaciari *et al.*, 1996) was the first to point out the significance of *Helicosphaera walbersdorfensis* for the biostratigraphic classification of the Miocene. In R-13 and W-11, *H. walbersdorfensis* occur sporadically throughout the profiles.

Gartner (1992) and Rafi *et al.* (1995; see also Fornaciari *et al.*, 1996) indicated the potential usefulness of the disappearance of *Calcidiscus premacintyreii* for subdividing the long interval between the LO of *S. heteromorphus* and the FO of *C. coalithus* (NN6–NN7). In R-13 and W-1, *C. premacintyreii* was extremely rare. Assemblages also consisted of species, such as *Braarudosphaera bigelowii*, *Coccolithus miopelagicus* ($> 14 \mu\text{m}$), *Discoaster deflandrei*, *Helicosphaera carteri*, *H. intermedia*, *Pontosphaera discopora*, *P. multipora*, *Reticulofenestra haqii*, *R. minuta*, *Sphenolithus abies*, *S. moriformis* and *Umblicosphaera rotula*, also characteristic for this interval. Although *S. abies* was described from the NN6–NN7 interval in the Central Paratethys (Lehotayova and Molčikova, 1978, *vide* Garecka, 2014), in Mediterranean region this species was observed in NN4 (Theodoridis, 1984). Bukry (1973) assigned it to NN5, whereas Perch-Nielsen (1985) to the NN9 Zone. In both profiles investigated, single specimens of *Sphenolithus heteromorphus* were observed, presumably as a result of redeposition. According to Müller (1981, *vide* Garecka, 2014) *S. heteromorphus* can occur sporadically in the NN6 and NN7 zones. Specimens of *Catinaster coalithus* were absent. On the basis of these results, the studied deposits belonging to the Machów Fm were assigned to the undivided NN6–NN7 zones, although this composition of calcareous nannoplankton could even indicate the NN7 Zone, as was previously suggested by Oszczytko-Clowes *et al.* (2012; see also Oszczytko-Clowes in Krzywiec *et al.*, 2014).

Palaeoecology

For the purpose of palaeoecological interpretation, the relative abundance of individual nannofossils taxa was determined to show alterations in the dominance of different species. The estimated quantitative ratios of calcareous nannoplankton taxa showed a general character of the assemblages.

The assemblages from W-1 and R-13 were dominated by nearshore placoliths and shallow-water cribriliths and pentaliths. The former group was represented by *C. pelagicus*, *C. floridanus* and *R. pseudoumbilica* ($> 7 \mu\text{m}$). Andreyeva-Grigorovich (2002) viewed these species as a cold-water ecogroup, because significant concentrations of them or monnoassociations were observed only in the northern areas of the Atlantic and the polar waters of the Pacific and Indian oceans (McIntyre and Bé, 1970; Dmitrenko, 1993 *vide* Andreyeva-Grigorovich, 2002).

Rahman and Roth (1990) describe *C. pelagicus* as a long-ranging species, providing palaeoclimatic information for the Middle Miocene to the Pleistocene. During the early Cenozoic, it evolved in tropical areas and migrated towards the poles during the mid-Cenozoic (Haq and Lohmann, 1976). Recently *C. pelagicus* was considered to be a subpolar species, a so-called r-strategist that preferred cold (7–14 °C), eutrophic, nutrient-rich surface waters, with intense upwelling (McIntyre and Be, 1967; Spezzaferri and Ćorić, 2001). According to Cachão and Moita (2000), this traditional interpretation of *C. pelagicus* as a cold-water proxy does not fully explain its distribution patterns at the Western Iberian Margin. They suggest an extension of the optimum

living and maximum temperatures of *C. pelagicus* to 16 °C and 18 °C respectively, owing to its abundant occurrence in the upwelling system in waters of subtropical origin, although also related to the lowest temperatures. Cachão and Moita (2000) infer that its niche may be associated with moderate fronts of different origin (thermal, haline, confluence of distinct water bodies). It appears that this species is mainly a high-nutrient indicator, which can be used as a front tracer of the outer limits of productivity-enhanced areas (Cachão and Moita, 2000; Doláková *et al.*, 2014). Its resistance to carbonate dissolution might improve its relative frequency (Rahman and Roth, 1990).

According to Wei and Wise (1990), *C. floridanus* may be considered as temperate water form. It belongs to the long-ranging taxa, which occur in the Palaeogene and extend to the NN7 Zone (Young, 1998), hence its high abundance can be due to reworking.

R. pseudoumbilica and other related species seem to have no specific ecological preferences (Beaufort and Aubry, 1992). Usually, this species was regarded as cosmopolitan (Beaufort and Aubry, 1992, and references therein). During the Neogene, it was most common at mid and low latitudes (Haq, 1980).

The common occurrence of **cribriliths**, in both profiles represented by the genus *Pontosphaera*, may be indicative of shallower, marine environments (Bukry, 1971; Roth and Thierstein, 1972; see also Aubry, 1984) as may be the presence of **pentaliths**, such as *B. bigelowii* (Gran and Braarud, 1935). The preference of *B. bigelowii* for shallow waters has been related either to water depth (Takayama, 1972) or to lower salinity and higher turbulence (Aubry, 1984, and references therein). Blooms of *B. bigelowii* have been associated also with the influx of terrigenous material (Švábenická, 1999) and eutrophication (Cunha and Shimabukuro, 1997; see also Bartol *et al.*, 2008). Bartol *et al.* (2008) suggest that this species can thrive in unusual palaeoceanographic conditions and its high abundance is associated with an opportunistic response to reduced competition (Thierstein *et al.*, 2004). In both profiles, this species occurs with lower frequency, except in the upper part of the W-1 profile, where a significant enrichment in it was observed.

Representatives of *Helicosphaera* group (Perch-Nielsen, 1985) and small reticulofenestrids (Haq, 1980) were also interpreted as nearshore species. **Helicoliths** are abundant in shallow, eutrophic near-continental environments with an upwelling regime (Perch-Nielsen, 1985; see also Ćorić and Hohenegger, 2008). In both profiles, they were mostly represented by *H. carteri*. The geographic distribution of the living species in the Atlantic and the Pacific oceans seems to be dependent upon water temperature (Aubry, 1984, and references therein). Although *H. carteri* is eurythermal and tolerates temperature 5–30 °C (Okada and McIntyre, 1979), it is more common in tropical and subtropical nannoflora provinces, while it occurs less frequently in transitional, arctic and subarctic assemblages (Schneidermann, 1977).

Small reticulofenestrids were observed commonly in nannoflora along continental margins (Haq, 1980). Owing to ambiguous data about their ecological preferences, the interpretation of the causes of their blooms was unclear

(Holcová, 2013). Wade and Bown (2006) associated blooms of *R. minuta* with high environmental stress, as this species responds quickly to rapid changes and dominates in conditions, where other taxa cannot compete. It was considered to be a hardy, opportunistic taxon with wide ecological tolerance, but capable of flourishing in nutrient-rich conditions (Wade and Bown, 2006; see also Holcová, 2013). Wade and Bown (2006) pointed out that *R. minuta* may have tolerated brackish to hypersaline, high-productivity environments, which prevailed immediately prior to and following evaporites deposition. Some researchers regarded small reticulofenestrids as eutrophic species (Wells and Okada, 1997; Flores *et al.*, 1997; Bollmann *et al.*, 1998; Kameo, 2002; Wade and Bown, 2006), while others associated blooms of small *Reticulofenestra* with oligotrophic conditions and a well-stratified water column (Hallock, 1987; Beaufort and Aubry, 1992; Ćorić and Rögl, 2004; see also Holcová, 2013). Hallock (1987) indicated that sparse nutrient supplies in an oligotrophic environment necessitate smaller phytoplankton and longer, more complex food chains. Gartner *et al.* (1983) associated the size of the coccoliths with seasonal fluctuations in nutrients and temperature and suggested that the variation in relative abundance of small *R. minuta* is a result of changes in nutrient dynamics. According to Beaufort and Aubry (1992), *C. pelagicus* and *R. minuta* had opposite ecological affinities during the Miocene. On the basis of these relationships, Ćorić and Rögl (2004) calculated the percentage of *C. pelagicus* versus *R. minuta* (Cp/Rm ratio) and found a high correlation with *C. pelagicus* and the reworked taxa, together with a negative correlation with respect to *R. minuta*. In the majority of samples from the W-1 and R-13 boreholes, *C. pelagicus* strongly predominates quantitatively over small *R. minuta* and the percentage of clearly allochthonous species is relatively high. This is the result of strong erosion and turbulent water masses in an upwelling regime.

Warm-water **sphenoliths** were also common in oligotrophic, shallow environments (Perch-Nielsen, 1985; Andreyeva-Grigorovich, 2002; Ćorić and Hohenegger, 2008). In the W-1 and R-13 boreholes, *Sphenolithus* genus was represented by *S. moriformis* and rarer *S. abies*. Great concentrations of the former were observed in the tropical zones, whereas latter was most numerous in subtropical provinces (Dmitrenko, 1993, *vide* Andreyeva-Grigorovich, 2002). *C. miopelagicus* also was considered to be a palaeo-bioindicator for warm, oceanic waters (Aubry, 1984).

In both profiles, open oceanic **discoasters** are scarce or absent, which may confirm the shallow palaeoenvironment also documented by other taxa. Most of the *Discoaster* species had an ecological affinity for tropical and subtropical waters, except for *D. exilis* and *D. deflandrei*, which are either tolerant to or exhibit a preference for colder waters (Aubry, 1984; Rahman and Roth, 1990; Chira and Mărunteanu, 1999).

The interpretation of the clusters was carried out with reference to these palaeoecological preferences of calcareous nannoplankton. Nonmetrical Multidimensional Scaling (nMDS) was employed to illustrate the relations between the samples in a low-dimensional space. The degree of change in the composition of assemblages along the core

could be measured as the distances between subsequent samples, understood as the larger the distance, the stronger the species turnover (Ćorić and Hohenegger, 2008). Taking into account the relative abundances of individual taxa, the assemblages from both profiles seem to be similar. There is a clear predominance of nearshore eutrophic taxa, accompanied by a high percentage of redeposited species. It seems that the high availability of nutrients and non-stratified, turbulent water masses characterized the entire interval in both the R-13 and W-1 boreholes. The differences concern species, which occur with lower frequencies or do not have particular environmental preferences.

In **R-13**, Cluster 1, all species were observed in various proportions. Besides *C. pelagicus*, which is common in the whole profile, the nearshore helicoliths (*H. intermedia*, *H. walbersdorfensis*) and cribriliths (*P. multipora*) also characterize this cluster. The less frequently occurring *B. bigelowii*, *C. premacintyreii*, *C. miopelagicus* (> 14 µm), *C. nitescens*, *R. haqii*, *R. minuta*, *S. abies* and *U. rotula* have the highest indicator values of all classes. This cluster groups samples from the upper part of the core. Owing to preferences of the main species, it may indicate a shallow environment with a probable slight shift to oligotrophic conditions and higher temperature. Cluster 2 is characterized by a high proportion of *C. pelagicus*, *C. floridanus*, *D. deflandrei*, *H. carteri*, *R. pseudumbilica* (> 7 µm) and *S. moriformis*. This cluster may indicate a non-stratified water column with an upwelling regime. In Cluster 3, the main species are rare *P. discopora* and *C. macintyreii* occurring with irregular frequency. In addition, relatively high indicator values belong to *C. pelagicus* and *Helicosphaera* genus and very low ones to *R. minuta*, which could indicate near-shore eutrophic environments. The presence of *C. macintyreii* and helicoliths and the low number of discoasters according to Švábenická (2002) may be associated with an incipient transgression. Garecka and Olszewska (2011) mentioned possible restricted connections with the open seas, documented by the Mediterranean type of calcareous nannoplankton (see Piller *et al.*, 2007).

In the **W-1** borehole, Cluster 1 is characterized by the main species, such as *C. macintyreii*, *B. bigelowii*, *R. minuta*, *C. floridanus* and *U. rotula*. *B. bigelowii*, and small *R. minuta* were considered to be opportunistic species, appearing in conditions of high environmental stress. Cluster 2 contains only one sample, which differs significantly from the others, which is seen on the nMDS plot (Fig. 14). A lot of species are absent (Table 4). *S. abies* and close behind it *H. walbersdorfensis* demonstrate the highest indicator value in all of the species. Furthermore, *S. moriformis*, *R. minuta*, *C. nitescens* and *P. discopora* were the main species. All these species, except for *R. minuta*, occur relatively less commonly throughout the core. This cluster seems to indicate a shift to warmer conditions. In Cluster 3, the main species are *H. carteri*, *H. intermedia* and *P. multipora* and also rare *D. deflandrei* and *D. exilis*. The percentage of reworked species is high (Fig. 10). It indicates nearshore conditions. In Cluster 4, *C. pelagicus* dominates and together with helicoliths and cribriliths indicates an eutrophic environment. In this cluster, *R. minuta* reaches the lowest indicator value. Clusters 3 and 4 seem to indicate similar palaeoecological

conditions, which is seen on the nMDS plot where they are in tangential contacting. In Cluster 5, the high indicator values belong to *R. pseudoumbilica* ($> 7 \mu\text{m}$), *R. haqii* and *C. miopelagicus* ($> 14 \mu\text{m}$). This cluster seems to characterize intermediate conditions. *C. pelagicus*, helicoliths and cribriliths also are common; *R. minuta* is rarer.

CONCLUSIONS

On the basis of calcareous nannoplankton from the Rudka-13 and Wylewa-1 boreholes (Sieniawa–Rudka area), the deposits of the Machów Formation were assigned to the upper part of NN6 Zone and the NN7 Zone, corresponding to the Sarmatian. A definite determination of the NN7 biozone was problematic, owing to the absence of the rare zonal marker species *Discoaster kugleri*.

Reworked nanofossils were mostly of Eocene and Cretaceous ages. These results indicate that during the Sarmatian the PCFB was supplied with sediment both from the N (Cretaceous deposits of the Miechów Trough) and from the S (folded Miocene strata at the front of the Polish Outer Carpathians).

The results of quantitative analyses, based on the relative abundance of individual nanofossil taxa, indicate a shallow, coastal environment with a high nutrient supply. The estimated high number of allochthonous species and the presence of the damaged elements of coccoliths may indicate a strong supply of terrigenous material and unstable conditions in a shallow-water basin. The palaeoecological interpretation was based on the occurrence of such species as *C. pelagicus*, reticulofenestrads, cribriliths, pentoliths, helicoliths, sphenoliths, and discoasterids and on the percentage of reworked species. The assemblages were dominated by nearshore placolith and shallow-water cribriliths, whereas open-oceanic discoasterids occur infrequently, which indicates isolation of the basin. The high abundance of *C. pelagicus*, indicating eutrophic conditions, is correlated positively with the high percentage of reworked taxa, which can be associated with turbulent water masses and deposition near the shoreline. The low variation in composition of the calcareous nannoplankton assemblages from the R-13 and W-1 boreholes may indicate an environment with relatively minor changes.

The high percentage of reworked specimens and the presence of long-ranging taxa and taxa resistant to carbonate dissolution may have affected the palaeoecological interpretation.

Acknowledgements

We are grateful to the reviewers Danuta Peryt (Institute of Paleobiology, Polish Academy of Sciences, Warsaw, Poland) and Katarína Holcová (Institute of Geology and Palaeontology, Charles University Prague, Praha, Czech Republic) for their critical reviews and suggestions that helped us to improve our manuscript. Special thanks are due to Barbara Studencka (Museum of the Earth, Polish Academy of Sciences, Warsaw, Poland) for valuable discussion on stratigraphy and Patrycja Wójcik-Taboń (Institute of Geological Sciences, Jagiellonian University, Krakow, Poland) for assistance with the graphics. We also thank Paweł Filipiak

(Department of Palaeontology and Stratigraphy, University of Silesia, Katowice, Poland) for extensive editorial efforts and Frank Simpson (Department of Earth and Environmental Sciences, University of Windsor, ON Canada) for proofreading. This project was financially supported by the National Science Centre (Decision No. 2011/01/N/ST10/06656) and carried out at the Jagiellonian University, in the Institute of Geological Sciences. The Polish Oil and Gas Company kindly provided samples from the Wylewa-1 and Rudka-13 boreholes.

REFERENCES

- Abdul Aziz, H., Di Stefano, A., Foresi, L. M., Hilgen, F. J., Iaccarino, S. M., Kuiper, K. F., Lirer, F., Salvatorini, G. & Turco, E., 2008. Integrated stratigraphy and Ar-40/Ar-39 chronology of early Middle Miocene sediments from DSDP Leg 42A, Site 372 (Western Mediterranean). *Palaeogeography, Palaeoclimatology, Palaeoecology*, 257: 123–138.
- Alexandrowicz, S., Garlicki, A. & Rutkowski, J., 1982. Basic lithostratigraphic units of the Miocene deposits of the Carpathian Foredeep. *Kwartalnik Geologiczny*, 26: 470–471. [In Polish, with English summary.]
- Andreyeva-Grigorovich, A., 2002. Biostratigraphy and paleoecology of the upper Badenian and lower Sarmatian of the Carpathian foredeep on the basis of nannoplankton. *Bulletin de l'Académie Serbe des Sciences et des Arts*, 125: 75–82.
- Andreyeva-Grigorovich, A. S., Kulchytsky, Y. O., Gruzman, A. D., Lozynyak, P. Y., Petrashkevich, M. I., Portnyagina, L. O., Ivanina, A. V., Smirnov, S. E., Trofimovich, N. A., Savitskaya, N. A. & Shvareva, N. J., 1997. Regional stratigraphic scheme of Neogene formations of the Central Paratethys in the Ukraine. *Geologica Carpathica*, 48: 123–136.
- Andreyeva-Grigorovich, A. S., Oszczytko, N., Ślącza, A., Oszczytko-Clowes, M., Savitskaya, N. A. & Trofimovich, N., 2008. New data on the stratigraphy of the folded Miocene Zone at the front of the Ukrainian Outer Carpathians. *Acta Geologica Polonica*, 58: 325–353.
- Andreyeva-Grigorovich, A., Oszczytko, N., Ślącza, A., Savitskaya, N. & Trofimovich, N., 1999. The age of the Miocene salt deposits in the Wieliczka, Bochnia and Kalush areas (Polish and Ukrainian Carpathian Foredeep). *Biuletyn Państwowego Instytutu Geologicznego*, 387: 85–96.
- Andreyeva-Grigorovich, A. S., Oszczytko, N., Ślącza, A., Savitskaya, N. A. & Trofimovich, N. A., 2003. Correlation of the Late Badenian salts of the Wieliczka, Bochnia and Kalush areas (Polish and Ukrainian Carpathian Foredeep). *Annales Societatis Geologorum Poloniae*, 73: 67–89.
- Aubry, M. P., 1984. *Handbook of Cenozoic Calcareous Nannoplankton*. Book 1: Ortholithae (Discoasters), 266 pp. Book 2: Ortholithae (Holococcoliths, Ceratoliths and other), 279 pp. Book 3: Ortholithae (Pentaliths, and others), Heliolithae (Fasciculiths, Sphenoliths and others), 220 pp. Book 4: Heliolithae (Helicoliths, Cribriliths, Lopadoliths and others), 381 pp. Micropaleontology Press, American Museum of Natural History, New York.
- Báldi-Beke, M., 1982. *Helicosphaera mediterranea* Müller, 1981, in its stratigraphical importance in the Lower Miocene. *International Nannoplankton Association Newsletter*, 4: 104–106.
- Bartol, M., 2009. *Middle Miocene Calcareous Nannoplankton of NE Slovenia (Western Central Paratethys)*. Založba ZRC/ZRC Publishing, Ljubljana, 136 pp.
- Bartol, M., Pavšič, J., Dobnikar, M. & Bernasconi, S. M., 2008. Unusual *Braarudosphaera bigelowii* and *Micrantholithus vesper* enrichment in the Early Miocene sediments from the

- Slovenian Corridor, a seaway linking the Central Paratethys and the Mediterranean. *Palaeogeography, Palaeoclimatology, Palaeoecology*, 267: 77–88.
- Beaufort, L. & Aubry, M. P., 1992. Palaeoceanographic implications of a 17 m.y. long record of high-latitude Miocene calcareous nannoplankton fluctuations. *Proceeding of Ocean Drilling Program, Scientific Results*, 120: 530–549.
- Bollmann, J., Baumann, K. H. & Thierstein, H. R., 1998. Global dominance of *Gephyrocapsa* coccoliths in the late Pleistocene: Selective dissolution, evolution, or global environmental change? *Paleoceanography*, 13: 517–529.
- Bown, P. R. & Young, J. R., 1998. Techniques. In: Bown, P. R. (ed.), *Calcareous Nannofossil Biostratigraphy*. Kluwer Academic Publishers, Dordrecht, pp. 16–28.
- Bramlette, M. N. & Wilcoxon, J. A., 1967. Middle Tertiary calcareous nannoplankton of the Cipero Section, Trinidad. *Tulane Studies in Geology and Paleontology*, 5: 93–131.
- Bukry, D., 1971. Cenozoic calcareous nannofossils from the Pacific Ocean. *Transactions of the San Diego Society of Natural History*, 16: 303–326.
- Bukry, D., 1973. Low-latitude coccolith biostratigraphic zonation. *Deep Sea Drilling Project Reports*, 15: 685–703.
- Bukry, D. & Okada, H., 1980. Supplementary modification and biostratigraphic zonation (Bukry, 1973, 1975). *Marine Micropaleontology*, 5: 321–325.
- Cachão, M. & Moita, M. T., 2000. *Coccolithus pelagicus*, a productivity proxy related to moderate fronts of Western Iberia. *Marine Micropaleontology*, 39: 131–155.
- Chira, C. & Măruntanu, M., 1999. Middle Miocene (Lower Badenian) calcareous nannofossils from the Mureș passageway and Făget Basin, Romania. *Acta Palaeontologica Romaniaae*, 5: 73–82.
- Cicha, I., Rögl, F., Rupp, C. & Čtyroká, J., 1998. Oligocene-Miocene foraminifera of the Central Paratethys. *Abhandlungen der Senckenbergischen Naturforschenden Gesellschaft*, 549: 3–7.
- Cunha, A. A. S. & Shimabukuro, S., 1997. *Braarudosphaera* blooms and anomalous enrichments of Nannoconus: evidence from the Turonian South Atlantic, Santos Basin, Brazil. *Journal of Nannoplankton Research*, 19: 51–55.
- Czepiec, I., 1997. Sarmatian Foraminifera microfauna from the Carpathian Foredeep. *Kwartalnik AGH, Geologia*, 23: 357–275. [In Polish, with English summary.]
- Ćorić, S. & Hohenegger, J., 2008. Quantitative analyses of calcareous nannoplankton assemblages from the Baden-Sooss section (Middle Miocene of Vienna Basin, Austria). *Geologica Carpathica*, 59: 447–460.
- Ćorić, S. & Rögl, F., 2004. Roggendorf-1 borehole, a key-section for Lower Badenian transgressions and the stratigraphic position of the Grund Formation (Molasse Basin, Lower Austria). *Geologica Carpathica*, 55: 165–178.
- Ćorić, S. & Švábenická, L., 2004. Calcareous nannofossil biostratigraphy of the Grund Formation (Molasse Basin, Lower Austria). *Geologica Carpathica*, 55: 147–153.
- De Leeuw, A., Bukowski, K., Krijgsman, W. & Kuiper, K. F., 2010. The age of the Badenian Salinity Crisis; impact of Miocene climate variability on the circum-Mediterranean region. *Geology*, 38: 715–718.
- Dmitrenko, O. B., 1993. *Biogeography of the Atlantic and Indian Oceans by Nannoplankton During Cenozoic*. Nauka, Moskva, 175 pp.
- Doláková, N., Holcová, K., Nehyba, S., Hladilová, Š., Brzobohatý, R., Zágorský, K., Hrabovský, J., Seko, M. & Utescher, T., 2014. The Badenian parastratotype at Židlochovice from the perspective of the multiproxy study. *Neues Jahrbuch für Geologie und Paläontologie, Abhandlungen*, 271: 169–201.
- Drooger, M. M., 1978. Statistics. In: Zacharias, W. J., Riedel, W. R., Sanfilippo, A., Schmidt, R. R., Broelsma, M. J., Schrader, H. J., Gersonde, R., Drooger, M. M. & Broekman, J. A. (eds), *Micropaleontological Counting Methods and Techniques: an Exercise on an Eight Metres Section of the Lower Pliocene of Capo Rossello, Sicily*. Utrecht Micropaleontological Bulletins, 17: 19–46.
- Dufrêne, M. & Legendre, P., 1997. Species assemblages and indicator species: the need for a flexible asymmetrical approach. *Ecological Monographs*, 67: 345–366.
- Flores, J. A., Sierro, F. S., Francés, G., Vasquez, A. & Zamarreno, I., 1997. The last 100,000 years in the western Mediterranean: Sea surface water and frontal dynamics as revealed by coccolithophores. *Marine Micropaleontology*, 29: 351–366.
- Foresi, L. M., Bonomo, S., Caruso, A., Di Stefano, A., Di Stefano, E., Iaccarino, S. M., Lirer, F., Mazzei, R., Salvatorini, G. & Sprovieri, R., 2002. High resolution calcareous plankton biostratigraphy of the Serravallian succession of the Tremiti Islands (Adriatic Sea, Italy). *Rivista Italiana di Paleontologia e Stratigrafia*, 108: 257–273.
- Fornaciari, E., Di Stefano, A., Rio, D. & Negri, A., 1996. Middle Miocene quantitative calcareous nannofossil biostratigraphy in the Mediterranean region. *Micropaleontology*, 42: 37–63.
- Fornaciari, E., Raffi, I., Rio, D., Villa, G., Backman, J. & Olafsson, G., 1990. Quantitative distribution patterns Oligocene and Miocene calcareous nannofossils from the western equatorial Indian Ocean. *Proceedings of the Ocean Drilling Program, Scientific Results*, 115: 237–254.
- Galloway, W. E., 1989. Genetic stratigraphic sequences in basin analysis II: application to northwest Gulf of Mexico Cenozoic basin: American Association of Petroleum Geologists Bulletin, 73: 143–154.
- Galović, I. & Young, J., 2012. Revised taxonomy and stratigraphy of Middle Miocene calcareous nannofossils of the Paratethys. *Micropaleontology*, 58: 305–334.
- Garecka, M., 2014. Biostratigraphy of Middle Miocene deposits in the Trojanowice 2 borehole based on calcareous nannoplankton investigations. *Biuletyn Państwowego Instytutu Geologicznego*, 459: 33–44. [In Polish, with English summary.]
- Garecka, M. & Jugowicz, M., 1999. Results of the biostratigraphic study of Miocene in the Carpathian Foredeep based on calcareous nanoplankton. *Prace Państwowego Instytutu Geologicznego*, 168: 29–42. [In Polish, with English summary.]
- Garecka, M., Marciniak, P., Olszewska, B. & Wójcik, A., 1996. New biostratigraphic data and attempt to correlation of the Miocene deposits in the basement of the Western Carpathians. *Przegląd Geologiczny*, 44: 495–501. [In Polish, with English summary.]
- Garecka, M. & Olszewska, B., 2011. Correlation of the Middle Miocene deposits in SE Poland and western Ukraine based on foraminifera and calcareous nannoplankton. *Annales Societatis Geologorum Poloniae*, 81: 309–330.
- Gartner, S., 1992. Miocene nannofossils chronology in the North Atlantic DSDP site 608. *Marine Micropaleontology*, 18: 307–331.
- Gartner, S., Chen, M. P. & Stanton, R. J., 1983. Late Neogene nannofossils biostratigraphy and paleoceanography of the northeastern Gulf of Mexico and adjacent areas. *Marine Micropaleontology*, 8: 17–50.
- Gaździcka, E., 1994. Nannoplankton stratigraphy of the Miocene deposits in Tarnobrzeg area (northeastern part of the Carpathian Foredeep). *Geological Quarterly*, 38: 553–570.
- Gran, H. H. & Braarud, T., 1935. A quantitative study of the phytoplankton in the Bay of Fundy and the Gulf of Maine (includ-

- ing observations on hydrography, chemistry and turbidity). *Journal of the Biological Board of Canada*, 1 (5): 279–467.
- Hallock, P., 1987. Fluctuations in the trophic resource continuum: a factor in global diversity cycles? *Paleoceanography*, 2: 457–471.
- Hammer, Ř., Harper, D. A. T. & Ryan, P. D., 2001. PAST: Paleontological Statistics Software Package for Education and Data Analysis. *Paleontologia Electronica*, 4: 9.
- Haq, B. U., 1980. Biogeographic history of the Miocene calcareous nannoplankton and paleoceanography of the Atlantic Ocean. *Micropaleontology*, 26: 414–443.
- Haq, B. U. & Lohmann, G. P., 1976. Early Cenozoic calcareous nannoplankton biogeography of the Atlantic Ocean. *Marine Micropaleontology*, 1: 119–194.
- Hay, W. W., 1970. Calcareous nannofossils from cores recovered on Leg 4. *Initial Report Deep Sea Drilling Project*, 4: 455–501.
- Hilgen, F. J., Abdul-Aziz, H., Krijgsman, W., Raffi, I. & Turco, E., 2003. Integrated stratigraphy and astronomical tuning of Serravallian and lower Tortonian at Monte dei Corvi (Middle–Upper Miocene, northern Italy). *Palaeogeography, Palaeoclimatology, Palaeoecology*, 199: 229–264.
- Hohenegger, J., Ćorić, S. & Wagreich, M., 2011. Beginning and division of the Badenian stages (Middle Miocene, Paratethys). In: Baĳ, M., Kaminski, M. A. & Wařkowska, A. (eds), *Integrating Microfossil Records from the Oceans and Epicontinental Seas. Grzybowski Foundation Special Publication*, 17: 92–93.
- Hohenegger, J., Ćorić, S. & Wagreich, M., 2014. Timing of the Middle Miocene Badenian Stage of the Central Paratethys. *Geologica Carpathica*, 65: 55–66.
- Hohenegger, J., Rögl, F., Ćorić, S., Pervesler, P., Lirer, F., Roetzel, R., Scholger, R. & Stingl, K., 2009. The Styrian Basin: a key to the Middle Miocene (Badenian/ Langhian) Central Paratethys transgressions. *Austrian Journal of Earth Sciences*, 102: 102–132.
- Holcová, K., 2013. Morphological variability of the Paratethyan Oligocene-Miocene small reticulofenestrid coccolithes and its paleoecological and paleogeographical implications. *Acta Palaeontologica Polonica*, 58: 651–668.
- Jasionowski, M., 1997. Outline of the lithostratigraphy of the Miocene deposits of the eastern part of the Carpathian Foredeep. *Biuletyn Państwowego Instytutu Geologicznego*, 375: 43–60. [In Polish, with English summary.]
- Jasionowski, M. & Peryt, T., 2004. Zapadlisko przedkarpackie – historia badań. In: Peryt, T. M. & Piwocki, M. (eds), *Budowa geologiczna Polski, t. 1. Stratygrafia, cz. 3a. Kenozoik–paleogen–neogen*. Państwowy Instytut Geologiczny, Warszawa, pp. 203–211. [In Polish.]
- Jurkiewicz, H. & Karnkowski, P., 1961. Tortonian Spirialis Horizon within the Carpathians Foreland. *Przegląd Geologiczny*, 9: 24–27. [In Polish, with English summary.]
- Kameo, K., 2002. Late Pliocene Caribbean surface water dynamics and climatic changes based on calcareous nannofossil records. *Palaeogeography, Palaeoclimatology, Palaeoecology*, 179: 211–226.
- Kováč, M., Andreyeva-Grigorovich, A., Bajraktarević, Z., Brzobohatý, R., Filipescu, S., Fodor, L., Harzhauser, M., Oszczytko, N., Nagymarosy, A., Pavelić, D., Rögl, F., Saftić, B., Sliva, L. & Studencka, B., 2007. Badenian evolution of the Central Paratethys Sea: paleogeography, climate and eustatic sea level changes. *Geologica Carpathica*, 58: 479–606.
- Krzywiec, P., Aleksandrowski, P., Ryzner-Siupik, B., Papiernik, B., Siupik, J., Mastalerz, K., Wysocka, A. & Kasiński, J., 2005. Geological structure and origin of the Miocene Ryszkowa Wola Horst (Sieniawa–Rudka area, eastern part of the Carpathian Foredeep Basin) – Results of 3D seismic data interpretation. *Przegląd Geologiczny*, 53: 656–663. [In Polish, with English summary.]
- Krzywiec, P., Oszczytko, N., Bukowski, K., Oszczytko-Clowes, M., Śmigielski, M., Stuart, F. M., Persano, C. & Sinclair, H. D., 2014. Structure and evolution of the Carpathian thrust front between Tarnów and Pilzno (Pogórska Wola area, southern Poland) – results of integrated analysis of seismic and borehole data. *Geological Quarterly*, 58: 409–426.
- Krzywiec, P., Wysocka, A., Oszczytko, N., Mastalerz, K., Papiernik, B., Wróbel, G., Oszczytko-Clowes, M., Aleksandrowski, P., Madej, K. & Kijewska, S., 2008. Evolution of the Miocene deposits of the Carpathian Foredeep in the vicinity of Rzeszów (the Sokołów–Smolarzyny 3D seismic survey area). *Przegląd Geologiczny*, 56: 232–244. [In Polish, with English summary.]
- Legendre, P., 2013. Indicator species: computation. In: Levin, S. (ed.), *Encyclopedia of Biodiversity, 2nd edition*. Academic Press, Waltham, MA, USA, pp. 264–268.
- Lehotayova, R. & Molčikova, V., 1978. Die nannofossilien des Badenien. Das Nannoplankton in der Tschechoslowakei. In: Papp, A., Cicha, I., Seneř, J. & Steininger, F. (eds), *Chronostratigraphie und Neostatratotypen. Miozän der Zentralen Paratetyts. Bd. VI. M₄ Badenien (Moravien, Wielicien, Kosovien)*, Vydavateľstvo Slovenskej Akadémie Vied, Bratislava, pp. 481–486.
- Łomnicki, J., 1897. Iły krakowieckie. *Kosmos*, 22: 571–578. [In Polish.]
- Łuczowska, E., 1964. Stratygrafia mikropaleontologiczna miocenu w rejonie Tarnobrzeg-Chmielnik. *Prace Geologiczne Komisji Komitetu Nauk Geologicznych Polskiej Akademii Nauk, Oddział w Krakowie*, 20: 1–52. [In Polish.]
- Łuczowska, E., 1972. Facjostratotyp sarmatu facji przybrzeżnej na Roztoczu Lubelskim. *Sprawozdania z Posiedzeń Komisji Naukowych Polskiej Akademii Nauk*, 16: 224–226. [In Polish.]
- Martini, E., 1971. Standard Tertiary and Quaternary calcareous nannoplankton zonation. *Proceedings of the II Planktonic Conference. Roma 1970*. Edizioni Tecnoscienza, Rome, pp. 729–785.
- Martini, E. & Worsley, T., 1970. Standard Neogene calcareous nannoplankton zonation. *Nature*, 225: 289–290.
- Mastalerz, K., Wysocka, A., Krzywiec, P., Kasiński, J., Aleksandrowski, P., Papiernik, B., Ryzner-Siupik, B. & Siupik, J., 2006. Miocene succession at the Ryszkowa Wola high (Sieniawa–Rudka area), Carpathian Foredeep Basin: facies and stratigraphic interpretation of wellbore and 3D seismic data. *Przegląd Geologiczny*, 54: 333–342. [In Polish, with English summary.]
- McIntyre, A. & Bě, A. W. H., 1967. Modern *Coccolithophoridae* of the Atlantic Ocean. I. Placolith and cyrtholiths. *Deep Sea Research*, 14: 561–597.
- McIntyre, A. & Bě, A. W. H., 1967. Modern Pacific coccolithophorida: a paleontological thermometer. *Transactions of the New York Academy of Sciences*, 11: 720–731.
- Müller, C., 1981. Beschreibung neuer Helicosphaera- Arten aus dem Miozän und Revision biostratigraphischer Reichweiten einiger neogener Nannoplankton-Arten. *Senckenbergiana Lethaea*, 61: 427–35.
- Nagymarosy, A., 1985. The correlation of the Badenian in Hungary based on nannofloras. *Annales Universitatis Scientiarum Budapestiensis de Rolando Eötvös Nominata, Separatum Sectio Geologica*, 25: 33–86.
- Nejbert, K., Śliwiński, M. G., Layer, P., Olszewska-Nejbert, D., Babel, M., Gařiewicz, A. & Schreiber, B. C., 2010. Ar40/Ar39 dating of a Badenian tuff from the Babczyn-2 core

- (near Lubaczów, Polish Carpathian Foredeep) and its palaeogeographic and stratigraphic significance. *Mineralia Slovaca*, 42, p. 515.
- Ney, R., 1968. The role of the "Cracow Bolt" in the geological history of the Carpathian Foredeep and in the distribution of oil and gas deposits. *Prace Geologiczne Komisji Komitetu Nauk Geologicznych PAN, Oddział w Krakowie*, 45: 1–82. [In Polish, with English summary.]
- Ney, R., 1969. The Miocene of the southern Roztocze between Horyniec and Łówcza and of the adjacent area of the Carpathian Foredeep. *Prace Geologiczne Komisji Komitetu Nauk Geologicznych PAN, Oddział w Krakowie*, 60: 1–78. [In Polish, with English summary.]
- Ney, R., Burzewski, W., Bachleda, T., Górecki, W., Jakóbczak, K. & Słupczyński, K., 1974. Outline of paleogeography and evolution of lithology and facies of Miocene Layers on the Carpathian Foredeep. *Prace Komisji Geologicznej Komitetu Nauk Geologicznych PAN, Oddział w Krakowie*, 82: 1–65. [In Polish, with English summary.]
- Odrzywolska-Bieńkowska, E., 1966. Micropaleontological stratigraphy of the Miocene in the north-eastern margin of the Carpathian Foredeep. *Kwartalnik Geologiczny*, 10: 432–441. [In Polish, with English summary.]
- Odrzywolska-Bieńkowska, E., 1972. Micropaleontological stratigraphy of the younger tertiary in the borehole Dzwola, Roztocze area. *Kwartalnik Geologiczny*, 16: 669–675. [In Polish, with English summary.]
- Okada, H. & McIntyre, A., 1979. Seasonal distribution of modern coccolithophores in the western North Atlantic Ocean. *Marine Biology*, 54: 319–328.
- Olafsson, G., 1989. Quantitative calcareous nannofossil biostratigraphy of Upper Oligocene to Middle Miocene sediment from ODP Hole 667A and Middle Miocene sediment from DSDP Site 574. In: Ruddiman, W. F., Sarnthein, M., Backman, J., Baldauf, J. G., Curry, W., DuPont, L. M., Janecek, T., Pokras, E. M., Raymo, M. E., Stabell, B., Stein, R. & Thiermann, R. (eds), *Proceedings of the Ocean Drilling Program, Scientific Results, College Station, TX (Ocean Drilling Program)*, 108: 9–22.
- Olszewska, B., 1999. Biostratigraphy of Neogene in the Carpathian Foredeep in the light of new micropalaeontological data. *Prace Państwowego Instytutu Geologicznego*, 168: 9–28. [In Polish, with English summary.]
- Oszczypko, N., 1998. The Western Carpathian Foredeep – development of the foreland basin in front of the accretionary wedge and its burial history (Poland). *Geologica Carpathica*, 49: 415–431.
- Oszczypko, N., 1999. The Miocene subsidence of the Polish Carpathian Foredeep. *Prace Państwowego Instytutu Geologicznego*, 168: 209–230. [In Polish, with English summary.]
- Oszczypko, N., 2006. Development of the Polish sector of the Carpathian Foredeep. *Przegląd Geologiczny*, 54: 396–403. [In Polish, with English summary.]
- Oszczypko, N., Krzywiec, P., Popadyuk, I. & Peryt, T., 2006. Carpathian Foredeep Basin (Poland and Ukraine): its sedimentary, structural and geodynamic evolution. In: Golonka, J. & Picha, F. J. (eds), *The Carpathians and their foreland: geology and hydrocarbon resources. American Association of Petroleum Geologists Memoir*, 84: 293–350.
- Oszczypko, N. & Oszczypko-Clowes, M., 2012. Stages of development in the Polish Carpathian Foredeep Basin. *Central European Journal of Geosciences*, 4: 138–162.
- Oszczypko, N. & Ślącza, A., 1985. An attempt to palinspastic reconstruction of Neogene basins in the Carpathian Foredeep. *Annales Societatis Geologorum Poloniae*, 55: 55–76.
- Oszczypko-Clowes, M., Lelek, D. & Oszczypko, N., 2012. Sarmatian paleoecological environment of the Machów Formation based on the quantitative nannofossil analysis – a case study from the Sokółów area (Polish Carpathian Foredeep). *Geologica Carpathica*, 63: 267–294.
- Oszczypko-Clowes, M., Oszczypko, N. & Wójcik, A., 2009. New data on the late Badenian–Sarmatian deposits of the Nowy Sacz Basin (Magura Nappe, Polish Outer Carpathians) and their palaeogeographical implications. *Geological Quarterly*, 53: 273–292.
- Paruch-Kulczycka, J., 1999. Genus *Silicoplacentina* (Class Amoebina) from the Miocene Machów Formation (Krakowiec Clays) of the northern Carpathian Foredeep. *Geological Quarterly*, 43: 499–508. [In Polish, with English summary.]
- Pawłowski, S., Pawłowska, K. & Kubica, B., 1985. Geology of the Tarnobrzeg native sulphur deposit. *Prace Państwowego Instytutu Geologicznego*, 114: 1–109. [In Polish, with English summary.]
- Perch-Nielsen, K., 1985. Cenozoic calcareous nannofossils. In: Bolli, H. M., Saunders, J. B. & Perch-Nielsen, K. (eds), *Plankton Stratigraphy*. Cambridge University Press, Cambridge, pp. 427–554.
- Peryt, D., 1997. Calcareous nannoplankton stratigraphy of the Middle Miocene in the Gliwice area (Upper Silesia, Poland). *Bulletin of the Polish Academy of Sciences, Earth Sciences*, 45: 119–131.
- Peryt, D., 1999. Calcareous nannoplankton assemblages of the Badenian evaporites in the Carpathian Foredeep. *Biuletyn Państwowego Instytutu Geologicznego*, 387: 158–161.
- Peryt, D. & Gedl, P., 2010. Palaeoenvironmental changes preceding the Middle Miocene Badenian salinity crisis in the northern Polish Carpathian Foredeep Basin (Borków quarry) inferred from foraminifers and dinoflagellate cysts. *Geological Quarterly*, 54: 487–508.
- Peryt, T., 2006. Deposition of Middle Miocene Badenian evaporites in the Carpathian Foredeep Basin. *Przegląd Geologiczny*, 54: 438–444. [In Polish, with English summary.]
- Peryt, T. M., Jasionowski, M., Karoli, S., Petrichenko, O. I., Pobereski, A. V. & Turchinow, I. I., 1998. Correlation and sedimentary history of the Badenian gypsum in the Carpathian Foredeep (Ukraine, Poland, and Czech Republic). *Przegląd Geologiczny*, 46: 729–732. [In Polish, with English summary.]
- Peryt, T. M., Karoli, S., Peryt, D., Petrichenko, O. I., Gedl, P., Narkiewicz, W., Durkovi čova, J. & Dobieszyńska, Z., 1997. Westernmost occurrence of the Middle Miocene Badenian gypsum in central Paratethys (Kobeřice, Moravia, Czech Republic). *Slovak Geological Magazine*, 3: 105–120.
- Piller, W. E., Harzhauser, M. & Mandic, O., 2007. Miocene Central Paratethys stratigraphy – current status and future directions. *Stratigraphy*, 4: 151–168.
- Piwocki, M., Olszewska, B. & Czapowski, G., 1996. Korelacja litostratygraficzna neogenu Polski z krajami sąsiednimi. In: Malinowska, L. & Piwocki, M. (eds), *Budowa geologiczna Polski, t. III, Atlas skamieniałości przewodnich i charakterystycznych, 3a: Kenozoik–trzeciorzęd–neogen*, Państwowy Instytut Geologiczny, Warszawa, pp. 517–529. [In Polish.]
- Popov, S. V., I. G. Shcherba, L. B. Ilyina, L. A. Neveeskaya, N. P. Paramonova, S. O. Khondkarian & Magyar, I., 2006. Late Miocene to Pliocene palaeogeography of the Paratethys and its relation to the Mediterranean. *Palaeogeography, Palaeoclimatology, Palaeoecology*, 238: 91–106.
- Porębski, S. & Oszczypko, N., 1999. Lithofacies and origin of the Bogucice sands (Upper Badenian), Carpathian Foredeep, Poland. *Prace Państwowego Instytutu Geologicznego*, 168: 57–82. [In Polish, with English summary.]

- Raffi, I. & Flores, J. A., 1995. Pleistocene through Miocene calcareous nannofossils from eastern equatorial Pacific Ocean. In: Pisas, N. G., Mayer, L. A., Janecek, T. R., Palmer-Julson, A. & van Andel, T. H. (eds), *Proceedings of the Ocean Drilling Program, Scientific Results, College Station*, 138: 233–286.
- Raffi, I., Rio, D., d'Atri, A., Fornaciari, E. & Rocchetti, S., 1995. Quantitative distribution patterns and biomagnetostratigraphy of middle and late Miocene calcareous nannofossils from equatorial Indian and Pacific oceans (Leg 115, 130, and 138). In: Pisas, N. G., Mayer, L. A., Janecek, T. R., Palmer-Julson, A. & van Andel, T. H. (eds), *Proceedings Ocean Drilling Program, Scientific Results*, 138: 479–502.
- Rahman, A. & Roth, P. H., 1990. Late Neogene paleoceanography and paleoclimatology of the Gulf of Aden region based on calcareous nannofossils. *Paleoceanography*, 5: 91–107.
- Roth, P. H. & Thierstein, H., 1972. Calcareous nannoplankton: leg 14 of the Deep Sea Drilling Project. In: Hayes, D. E. & Pimm, A. C. (eds), *Initials Reports Deep Sea Drilling Project*, 14: 421–485.
- Rögl, F., 1998. Paleogeographic considerations for Mediterranean and Paratethys seaways (Oligocene to Miocene). *Annalen des Naturhistorischen Museums in Wien*, 99A: 279–310.
- Schneidermann, N., 1977. Selective dissolution of Recent coccoliths in the Atlantic Ocean. In: Ramsay, A. T. S. (ed.), *Oceanic Micropaleontology*. Academic Press, London, pp. 1009–1053.
- Spezzaferri, S. & Ćorić, S., 2001. Ecology of Karpatian (early Miocene) foraminifers and calcareous nannoplankton From Laa an der Thaya, Lower Austria: a statistical approach. *Geologica Carpathica*, 52: 361–374.
- Studencka, B. & Jasionowski, M., 2011. Bivalves from the Middle Miocene reefs of Poland and Ukraine: A new approach to Badenian/Sarmatian boundary in the Paratethys. *Acta Geologica Polonica*, 6: 79–114.
- Švábenická, L., 1999. *Braarudosphaera*-rich sediments in the Turonian of the Bohemian Cretaceous Basin, Czech Republic. *Cretaceous Research*, 20: 773–782.
- Švábenická, L., 2002. Calcareous nannofossils of the Upper Karpatian and Lower Badenian deposits in the Carpathian Foredeep, Moravia (Czech Republic). *Geologica Carpathica*, 53: 197–210.
- Śliwiński, M., Bąbel, M., Nejbart, K., Olszewska-Nejbart, D., Gašiewicz, A., Schreiber, B. C., Benowitz, J. A. & Layer, P., 2012. Badenian-Sarmatian chronostratigraphy in the Polish Carpathian Foredeep. *Palaeogeography, Palaeoclimatology, Palaeoecology*, 326–328: 12–29.
- Takayama, T., 1972. A note on the distribution of *Braarudosphaera bigelowii* (Gran and Braarud) Deflandre in the bottom sediments of Sendai Bay, Japan. *Transactions of the Paleontological Society of Japan, New Series*, 87: 429–435.
- Theodoridis, S. A., 1984. Calcareous nannofossils of the Miocene and revision of the helicoliths and discoasters. *Utrecht Micropaleontological Bulletins*, 32: 1–271.
- Thierstein, H. R., Cortés, M. Y. & Haidar, A. T., 2004. Plankton community behavior on ecological and evolutionary time-scale: when models confront evidence. In: Thierstein, H. R. & Young, J. (eds), *Coccolithophores, from Molecular Processes to Global Impact*. Springer, Berlin, pp. 455–479.
- Thierstein, H. R., Geitzenauer, K. R. & Molfino, B., 1977. Global synchronicity of late Quaternary coccolith datum levels: Validation by oxygen isotopes. *Geology*, 5: 400–405.
- Turco, E., Bambini, A. M., Foresi, L., Iaccarino, S., Lirer, F., Mazzei, R. & Salvatorini, G., 2002. Middle Miocene high-resolution calcareous plankton biostratigraphy at Site 926 (Leg 154, equatorial Atlantic Ocean). *Palaeoecological and palaeobiogeographical implications*. *Geobios*, 35 (Supplement 1): 257–276.
- Wade, B. S. & Bown, P. R., 2006. Calcareous nannofossils in extreme environments: the Messinian Salinity Crisis, Polemi Basin, Cyprus. *Palaeogeography, Palaeoclimatology, Palaeoecology*, 233: 271–286.
- Ward, J. H. Jr., 1963. Hierarchical grouping to optimize an objective function. *Journal of the American Statistical Association*, 58: 236–244.
- Watkins, D. K., 2007. Quantitative analysis of the calcareous nannofossil assemblages from CIROS-1, Victoria Land Basin, Antarctica. *Journal of Nannoplankton Research*, 29: 130–137.
- Wei, S. & Wise, W., 1990. Biogeographic gradients of the middle Eocene-Oligocene calcareous nanoplankton in the South Atlantic Ocean. *Palaeogeography, Palaeoclimatology, Palaeoecology*, 79: 29–61.
- Wells, P. & Okada, H., 1997. Response of nannoplankton to major changes in sea-surface temperature and movements of hydrological fronts over Site DSDP 594 (south Chatham Rise, southeastern New Zealand), during the last 130 kyr. *Marine Micropaleontology*, 32: 341–363.
- Young, J. R., 1998. Neogene. In: Bown, P. R. (ed.), *Calcareous Nannofossil Biostratigraphy*. Kluwer Academic Publishers, Dordrecht, pp. 225–265.

Appendix

An alphabetical list of calcareous nannoplankton species

- Blackites spinosus* (Deflandre et Fert 1954) Hay et Towe 1962
Braarudosphaera bigelowii (Gran et Braarud 1935) Deflandre 1947
Calcidiscus leptoporus (Murray et Blackman 1898) Loeblich et Tappan 1978
Calcidiscus macintyreii (Bukry et Bramlette 1969) Loeblich et Tappan 1978
Calcidiscus premacintyreii Theodoridis 1984
Chiasmolithus altus Bukry et Percival 1971
Chiasmolithus bidens (Bramlette et Sullivan 1961) Hay et Mohler 1967
Chiasmolithus expansus (Bramlette et Sullivan 1961) Gartner 1970
Chiasmolithus gigas (Bramlette et Sullivan 1961) Radomski 1968
Chiasmolithus grandis (Bramlette et Riedel 1954) Radomski 1968
Chiasmolithus medius Perch-Nielsen 1971
Chiasmolithus modestus Perch-Nielsen 1971
Chiasmolithus oamaruensis (Deflandre in Deflandre et Fert 1954) Hay, Mohler et Wade 1966
Chiasmolithus solitus (Bramlette et Sullivan 1961) Hay, Mohler et Wade 1966
Coccolithus miopelagicus (> 14 µm) Bukry 1971
Coccolithus pelagicus (Wallich 1877) Schiller 1930
Coronocyclus nitescens (Kamptner 1963) Bramlette et Wilcoxon 1967
Cyclicargolithus abisectus (Muller 1970) Wise 1973
Cyclicargolithus floridanus (Roth et Hay in Hay et al. 1967) Bukry 1971
Cyclicargolithus luminis (Sullivan 1965) Bukry 1971
Dictyococcites bisectus (Hay, Mohler et Wade 1966) Bukry et Percival 1971
Dictyococcites scrippsae Bukry et Percival 1971
Discoaster barbadiensis Tan Sin Hok 1927
Discoaster binodosus Martini 1958
Discoaster deflandrei Bramlette et Riedel 1954
Discoaster exilis Martini et Bramlette 1963
Discoaster lodoensis Bramlette et Riedel 1954
Discoaster multiradiatus Bramlette et Riedel 1954

- Discoaster saipanensis* Bramlette et Riedel 1954
Discoaster tanii Bramlette et Riedel 1954
Discoaster tanii nodifer Bramlette et Riedel 1954
Ellipsolithus distichus (Bramlette et Sullivan 1961) Sullivan 1964
Ellipsolithus macellus (Bramlette et Sullivan 1961) Sullivan 1964
Ericsonia fenestrata (Deflandre et Fert 1954) Stradner in Stradner et Edwards 1968
Ericsonia formosa (Kamptner, 1963) Haq 1971
Ericsonia robusta (Bramlette et Sullivan 1961) Edwards et Perch-Nielsen 1975
Ericsonia subdisticha (Roth et Hay in Hay *et al.* 1967) Roth in Baumann et Roth 1969
Helicosphaera ampliaperata Bramlette et Wilcoxon 1967
Helicosphaera bramlettei (Müller, 1970) Jafar et Martini 1975
Helicosphaera carteri (Wallich, 1877) Kamptner 1954
Helicosphaera compacta Bramlette et Wilcoxon 1967
Helicosphaera euphratis Haq 1966
Helicosphaera gartneri Theodoridis 1984
Helicosphaera heezenii (Bukry 1971) Jafar et Martini 1975
Helicosphaera intermedia Martini 1965
Helicosphaera lophota (Bramlette et Sullivan 1961) Locker 1973
Helicosphaera mediterranea Müller 1981
Helicosphaera recta (Haq, 1966) Jafar et Martini 1975
Helicosphaera reticulata Bramlette et Wilcoxon 1967
Helicosphaera scissura Müller 1981
Helicosphaera walbersdorfensis Müller 1974
Helicosphaera waltrans Theodoridis 1984
Heliolithus kleinpelli Sullivan 1964
Isthmolithus recurvus Deflandre in Deflandre et Fert 1954
Lanternithus minutus Stradner 1962
Neococcolithes dubius (Deflandre in Deflandre et Fert 1954) Black 1967
Pontosphaera discopora Schiller 1925
Pontosphaera latelliptica (Báldi-Beke et Baldi 1974) Perch-Nielsen 1984
Pontosphaera multipora (Kamptner ex Deflandre 1959) Roth 1970
Pontosphaera plana (Bramlette et Sullivan 1961) Haq 1971
Pontosphaera rothi Haq 1971
Reticulofenestra daviesii (Haq 1968) Haq 1971
Reticulofenestra dictyoda (Deflandré in Deflandré et Fert 1954) Stradner in Stradner et Edwards 1968
Reticulofenestra haqii Backman 1978
Reticulofenestra hillae Bukry et Percival 1971
Reticulofenestra lockerii Müller 1970
Reticulofenestra ornata Müller 1970
Reticulofenestra pseudoumbilica ($> 7 \mu\text{m}$) (Gartner 1967) Gartner 1969
Reticulofenestra reticulata (Hay, Mohler et Wade 1966) Roth 1970
Reticulofenestra umbilica (Levin, 1965) Martini et Ritzkowski 1968
Reticulofenestra minuta Roth 1970
Rhabdosphaera procera Martini 1969
Semihololithus kerabyi Perch-Nielsen 1971
Sphenolithus abies Deflandre in Deflandre et Fert 1954
Sphenolithus belemnus Bramlette et Wilcoxon 1967
Sphenolithus calyculus Bukry 1985
Sphenolithus conicus Bukry 1971
Sphenolithus disbelemnus Fornaciari et Rio 1996
Sphenolithus dissimilis Bukry et Percival 1971
Sphenolithus editus Perch-Nielsen in Perch-Nielsen *et al.* 1978
Sphenolithus furcatolithoides Locker 1967
Sphenolithus heteromorphus Deflandre 1953
Sphenolithus moriformis (Brönnimann et Stradner 1960) Bramlette et Wilcoxon 1967
Sphenolithus obtusus Bukry 1971
Sphenolithus predistensus Bramlette et Wilcoxon 1967
Sphenolithus radians Deflandre in Grassé 1952
Sphenolithus spiniger Bukry 1971
Sphenolithus strigosus Bown et Dunkley Jones 2006
Toweius callosus Perch-Nielsen 1971
Toweius eminens (Bramlette et Sullivan 1961) Perch-Nielsen 1971
Toweius rotundus Perch-Nielsen in Perch-Nielsen *et al.* 1978
Transversopontis fibula Getha 1976
Transversopontis obliquipons (Deflandre in Deflandre et Fert 1954) Hay, Mohler et Wade 1966
Transversopontis pulcher (Deflandre in Deflandre et Fert 1954) Perch-Nielsen 1967
Transversopontis pulcheroides (Sullivan 1964) Báldi-Beke 1971
Tribrachiatulus orthostylus Shamrai 1963
Umbilicosphaera rotula (Kamptner 1956) Varol 1982
Zygrhablithus bijugatus (Deflandre in Deflandre et Fert 1954) Deflandre 1959

Appendix Table 1. Percentage abundance of autochthonous species in samples from the Rudka-13 borehole.

RUDKA-13	Miocene s.s. taxa												Taxa with their last occurrence during the Miocene																									
	<i>Calcidiscus macintyreii</i>	<i>Calcidiscus premachinyrei</i>	<i>Coccolithus miopelagicus</i> (> 14µm)	<i>Coronocyclus nitescens</i>	<i>Helicosphaera carteri</i>	<i>Helicosphaera intermedia</i>	<i>Helicosphaera walbersdorffensis</i>	<i>Reticulofenestra haqti</i>	<i>Reticulofenestra minuta</i>	<i>Reticulofenestra pseudonubtica</i> (< 7 µm)	<i>Sphenolithus abies</i>	<i>Umbilicosphaera rotula</i>	<i>Braarudosphaera bigelowii</i>	<i>Coccolithus pelagicus</i>	<i>Cyclargolithus floridanus</i>	<i>Discaster deflandrei</i>	<i>Pontosphaera discopora</i>	<i>Pontosphaera multipora</i>	<i>Sphenolithus moriformis</i>																			
	P	±	P	±	P	±	P	±	P	±	P	±	P	±	P	±	P	±	P	±																		
s. 1			2.7	0.9	0.7	0.5	0.3	0.3	0.7	0.5	0.3	0.3	1.7	0.7	3.7	1.1	7.7	1.5	1.3	0.7	7.7	1.5	8.3	1.6	0.3	0.3	3.3	1	3	1								
s. 2			3.3	1	1	0.6	1.7	0.7					2.7	0.9	4.3	1.2	2.7	0.9	0.7	0.5					11	1.8	12	1.9	0.7	0.5	1.7	0.7	2	0.8				
s. 3	0.3	0.3	1.7	0.7	1.7	0.7	3.3	1					1	0.6	3.3	1	9	1.7	1.7	0.7					12.7	1.9	9	1.7	0.3	0.3	0.7	0.5	1.3	0.7	4.7	1.2		
s. 4	0.7	0.5	5	1.3	0.7	0.5	1.7	0.7					0.7	0.5	2.7	0.9	3	1	7.3	1.5	0.3	0.3	1.3	0.7	7	1.5	5.7	1.3	0.3	0.3	0.3	0.3	4.3	1.2	2	0.8		
s. 5	0.3	0.3	3.3	1	0.3	0.3	0.3	0.3	0.3	0.3					0.3	0.3	1.7	0.7	9.3	1.7	0.7	0.5			12.3	1.9	6.7	1.4			0.7	0.5	1	0.6	4.3	1.2		
s. 6	0.7	0.5	1.7	0.7	3.3	1	1.7	0.7	1	0.6					2.7	0.9	2.3	0.9	5.7	1.3	1	0.6	0.3	0.3	7.3	1.5	6	1.4			0.3	0.3	3.3	1	3	1		
s. 7	1	0.6	1.3	0.7				2	0.8						1.3	0.7	2.3	0.9	5	1.3	1	0.6	0.3	0.3	0.3	0.3	13	1.9	6	1.4			0.3	0.3	3.3	1	3	1
s. 8			3.3	1	1	0.6	0.3	0.3	0.3	0.3	0.3	0.3	0.7	0.5	2	0.8	4	1.1	7	1.5	0.7	0.5			0.7	0.5	11	1.8	6.3	1.4	0.7	0.5			3.7	1.1	0.3	0.3
s. 9	0.3	0.3	1.3	0.7	1	0.6	1.7	0.7							0.3	0.3	2	0.8	8.7	1.6	0.3	0.3	0.7	0.5	11.7	1.9	6.7	1.4			1	0.6	1.7	0.7	5	1.3		
s. 10			0.3	0.3	0.3	0.3	0.3	0.3	0.3	0.3	0.3	0.3	0.3	0.3	1	0.6	3	1	11	1.8	0.7	0.5	0.3	0.3	11.7	1.9	10.3	1.8			0.3	0.3	3.7	1.1	3	1		
s. 11	0.3	0.3	1	0.6	0.7	0.5	0.7	0.5	1	0.6	1.3	0.7	0.3	0.3	0.3	0.3	2.3	0.9	9.3	1.7	0.3	0.3			11.3	1.8	5.7	1.3	0.7	0.5	0.3	0.3	3	1	1.7	0.7		
s. 12	0.3	0.3	0.3	0.3	1.7	0.7	3	1	0.3	0.3	0.3	0.3	0.3	0.3	0.7	0.5	2.3	0.9	11	1.8	1	0.6	0.3	0.3	12	1.9	9.3	1.7			0.7	0.5	2.7	0.9	1.7	0.7		
s. 13			0.3	0.3	0.7	0.5	0.3	0.3	0.3	0.3	0.3	0.3	0.3	0.3	0.3	0.3	2.3	0.9	6.7	1.4	0.3	0.3	0.3	0.3	11.7	1.9	7	1.5			0.7	0.5	2.7	0.9	1.7	0.7		
s. 14	0.3	0.3	4	1.1	0.3	0.3	1.3	0.7							2.3	0.9	5.3	1.3	7.7	1.5					15	2.1	8.3	1.6			0.3	0.3	1.3	0.7	2.7	0.9		
s. 15			1.3	0.7	0.3	0.3	2	0.8							1.7	0.7			6.3	1.4					14.3	2	11.7	1.9	0.3	0.3	1	0.6	3.7	1.1	2.3	0.9		
s. 16	0.3	0.3	2.7	0.9			1.7	0.7	0.3	0.3					0.7	0.5	1	0.6	9.3	1.7					1.3	0.7	11	1.8	8.7	1.6	0.3	0.3	2	0.8	4.7	1.2		
s. 17			0.7	0.5	0.3	0.3	2.3	0.9	0.3	0.3					1	0.6	0.7	0.5	6.3	1.4					0.7	0.5	12	1.9	8	1.6	0.3	0.3	1	0.6	1.7	0.7	1.7	0.7
s. 18			2	0.8	0.3	0.3	2.3	0.9	0.3	0.3					1.7	0.7	3.3	1	6.3	1.4	0.3	0.3			13	1.9	7	1.5			0.7	0.5	1.7	0.7	1.7	0.7		
s. 19	0.3	0.3	3.7	1.1	1.3	0.7	1.7	0.7							0.3	0.3	1	0.6	12.3	1.9					8.3	1.6	7.3	1.5	0.3	0.3	0.7	0.5	2.7	0.9	1.7	0.7		
s. 23	0.3	0.3	3.3	1			1	0.6	0.7	0.5					0.7	0.5	2	0.8	12.3	1.9	1.7	0.7			9.3	1.7	8.7	1.6			3.7	1.1	2.7	0.9				
s. 25	0.7	0.5	1	0.6	0.3	0.3	0.7	0.5	0.3	0.3					1	0.6	2.7	0.9	8.3	1.6					0.3	0.3	11.7	1.9	7	1.5			0.7	0.5	1.3	0.7	2	0.8
s. 26	1.3	0.7	1.7	0.7	1	0.6	1.7	0.7	0.3	0.3	1.3	0.7	2.3	0.9	3.3	1	10.3	1.8	0.3	0.3					1.7	0.7	10.3	1.8	10.7	1.8	0.3	0.3			2	0.8	1	0.6
s. 27	0.7	0.5	0.7	0.5	0.7	0.5	0.7	0.5	0.3	0.3	0.3	0.3	1	0.6	7.3	1.5	7.3	1.5	0.3	0.3					1	0.6	12.7	1.9	4.7	1.2	0.3	0.3	0.7	0.5	1.7	0.7	1.7	0.7
s. 29	5	1.3	2	0.8	1.7	0.7	1	0.6							3.3	1	6	1.4							14.7	2	7.3	1.5					1.3	0.7	2.7	0.9		
s. 30	0.3	0.3	1.3	0.7	0.7	0.5	2	0.8	1	0.6					1.3	0.7	2.7	0.9	9.3	1.7	0.3	0.3			9.7	1.7	8.7	1.6			0.3	0.3	1.7	0.7	6	1.4		
s. 31	1.3	0.7	2	0.8	0.7	0.5	1	0.6	1.3	0.7	0.3	0.3	0.7	0.5	3.3	1	5	1.3							0.7	0.5	11	1.8	7	1.5			1	0.6	1	0.6	1.3	0.7
s. 32	4	1.1	0.3	0.3											0.3	0.3	0.7	0.5	3.7	1.1	4.3	1.2	0.3	0.3	14	2	5.7	1.3					1.7	0.7	3	1		
s. 33	2	0.8	3.3	1											0.3	0.3	1.7	0.7	2.7	0.9	6.7	1.4	1.3	0.7	1	0.6	12.3	1.9	6	1.4			0.3	0.3	1.3	0.7	2	0.8

